The Pea TCP Transcription Factor PsBRC1 Acts Downstream of Strigolactones to Control Shoot Branching[1][W]

Nils Braun[2,3], Alexandre de Saint Germain[2], Jean-Paul Pillot, Stéphanie Boutet-Mercey, Marion Dalmais, Ioanna Antoniadi, Xin Li, Alessandra Maia-Grondard, Christine Le Signor, Nathalie Bouteiller[4], Da Luo, Abdelhafid Bendahmane, Colin Turnbull, and Catherine Rameau*

Institut Jean-Pierre Bourgin, INRA UMR1318 INRA-AgroParisTech, F–78000 Versailles, France (N. Braun, A.d.S.G., J.-P.P., S.B.-M., A.M.-G., C.R.); School of Life Sciences, Sun Yat Sen University, Guangzhou 510275, China (X.L., D.L.); Unité de Recherche en Génomique Végétale, INRA/CNRS, 91057 Evry cedex, France (M.D., N. Bouteiller, A.B.); INRA Dijon, 21065 Dijon cedex, France (C.L.S.); and Division of Cell and Molecular Biology, Imperial College London, London SW7 2AZ, United Kingdom (I.A., C.T.)

The function of *PsBRC1*, the pea (*Pisum sativum*) homolog of the maize (*Zea mays*) *TEOSINTE BRANCHED1* and the Arabidopsis (*Arabidopsis thaliana*) *BRANCHED1* (*AtBRC1*) genes, was investigated. The pea *Psbrc1* mutant displays an increased shoot-branching phenotype, is able to synthesize strigolactone (SL), and does not respond to SL application. The level of pleiotropy of the SL-deficient *ramosus1* (*rms1*) mutant is higher than in the *Psbrc1* mutant, *rms1* exhibiting a relatively dwarf phenotype and more extensive branching at upper nodes. The *PsBRC1* gene is mostly expressed in the axillary bud and is transcriptionally up-regulated by direct application of the synthetic SL GR24 and down-regulated by the cytokinin (CK) 6-benzylaminopurine. The results suggest that *PsBRC1* may have a role in integrating SL and CK signals and that SLs act directly within the bud to regulate its outgrowth. However, the *Psbrc1* mutant responds to 6-benzylaminopurine application and decapitation by increasing axillary bud length, implicating a *PsBRC1*-independent component of the CK response in sustained bud growth. In contrast to other SL-related mutants, the *Psbrc1* mutation does not cause a decrease in the CK zeatin riboside in the xylem sap or a strong increase in *RMS1* transcript levels, suggesting that the *RMS2*-dependent feedback is not activated in this mutant. Surprisingly, the double *rms1 Psbrc1* mutant displays a strong increase in numbers of branches at cotyledonary nodes, whereas branching at upper nodes is not significantly higher than the branching in *rms1*. This phenotype indicates a localized regulation of branching at these nodes specific to pea.

Early studies on shoot branching were based on decapitation experiments that emphasized the role of the shoot apex in the inhibition of axillary bud outgrowth (Thimann and Skoog, 1933). In the classical theory of apical dominance, auxin from the apex was proposed to act indirectly to suppress bud outgrowth, while cytokinin (CK) coming from the roots promoted bud outgrowth (Snow, 1937; Sachs and Thimann, 1967; Cline, 1991). More than a decade ago, with the identification and characterization of high-branching mutants in pea (*Pisum sativum*), Arabidopsis (*Arabidopsis thaliana*), rice (*Oryza sativa*), and *Petunia hybrida*, long-distance signaling was shown to be an important process in the control of shoot branching (Ongaro and Leyser, 2008; Beveridge et al., 2009; McSteen, 2009; Beveridge and Kyozuka, 2010). In pea, grafting revealed the existence of two novel long-distance signals controlling shoot branching that were different from auxin and CK (Beveridge et al., 2000, 2009; Beveridge, 2006): a root-to-shoot branching inhibitor (Beveridge et al., 1997b; Morris et al., 2001), which was subsequently identified as a strigolactone (SL) or derived compound (Gomez-Roldan et al., 2008; Umehara et al., 2008), and a shoot-to-root feedback signal, which was shown to be auxin independent and has still to be identified (Beveridge et al., 1997a, 2000). To date, the genetic and physiological model of branching control in pea includes five *RAMOSUS* genes (*RMS1–RMS5*). Branching of the pea SL-deficient *rms1* and *rms5* mutants is suppressed when scions of these mutants are grafted on wild-type rootstock or when the syn-

[1] This work was supported by the European Union FP6 Grain Legumes Integrated Project (to N. Braun, M.D., N. Bouteiller, A.B., C.L.S., and C.R.), the ERA-PG 027 COGS project (to N. Braun and C.R.), and the Ministère de l'Education Nationale, de la Recherche et de la Technologie (to A.d.S.G.).

[2] These authors contributed equally to the article.

[3] Present address: Université Pierre et Marie Curie, UR5 4 Place Jussieu, 75005 Paris, France.

[4] Present address: Institut Jean-Pierre Bourgin, INRA UMR1318 INRA-AgroParisTech, F–78000 Versailles, France.

* Corresponding author; e-mail catherine.rameau@versailles.inra.fr.

The author responsible for distribution of materials integral to the findings presented in this article in accordance with the policy described in the Instructions for Authors (www.plantphysiol.org) is: Catherine Rameau (catherine.rameau@versailles.inra.fr).

[W] The online version of this article contains Web-only data.

www.plantphysiol.org/cgi/doi/10.1104/pp.111.182725

thetic SL GR24 is applied on axillary buds. In contrast, the *rms3* and *rms4* SL-response mutants are not rescued when grafted to wild-type rootstocks, and they do not respond to GR24 application (Table I; Beveridge et al., 1996, 2009; Dun et al., 2009). All *rms* mutants, except *rms2*, have high levels of *RMS1* transcripts in epicotyls compared with the wild type (Foo et al., 2005). Moreover, these branching mutants, with the exception of *rms2*, have greatly reduced amounts of CK in xylem sap (X-CK) compared with wild-type plants (Table I; Beveridge et al., 1997a; Morris et al., 2001; Foo et al., 2007). The reduced X-CK in several *rms* branching mutants appears to be mediated by a shoot-to-root mobile signal (Beveridge et al., 1997a; Beveridge, 2000). Because *rms2* is the only *rms* mutant that does not show down-regulation of X-CK, it has been proposed that *RMS2* may play a role in the generation of this feedback signal. It was hypothesized that the same signal may also regulate *RMS1* transcript levels (Foo et al., 2005), because X-CK and *RMS1* transcript levels are typically anticorrelated (Dun et al., 2009). The *rms2* mutant does respond to SL (Dun et al., 2009). This mutant, having low transcript levels of *RMS1* and slightly elevated X-CK in comparison with the wild type, may branch because of low SL levels and/or high CK content.

Among these five *RMS* genes, three have been cloned and correspond to branching genes identified in other species. The *RMS1* and *RMS5* genes encode the CAROTENOID CLEAVAGE DIOXYGENASE (CCD) enzymes CCD8 and CCD7, respectively (Sorefan et al., 2003; Johnson et al., 2006). The *RMS4* gene encodes an F-box protein and corresponds to the Arabidopsis *MAX2* gene (Stirnberg et al., 2002; Johnson et al., 2006). While *RMS4* transcripts are found in all tissues, the SL biosynthesis *RMS1* and *RMS5* genes are highly expressed in roots and in the basal stem (Foo et al., 2005; Johnson et al., 2006) and were shown to be finely regulated along the stem (Dun et al., 2009).

In the current model of shoot branching in pea, auxin, originating from the main shoot apex, regulates SL levels by maintaining *RMS1* and *RMS5* transcript levels (Foo et al., 2005; Johnson et al., 2006) and down-regulates CK in both xylem sap (Bangerth, 1994; Li et al., 1995) and the stem (Tanaka et al., 2006). Auxin regulation of SL synthesis genes, and bud outgrowth inhibition by SL application in decapitated plants, suggest that SL is the second messenger by which auxin controls branching in decapitation experiments (Brewer et al., 2009). SL and CK would act locally within the axillary bud to control its outgrowth. Another hypothesis has been proposed where SLs would act upstream of auxin by modulating its transport in the main shoot by limiting the accumulation of PIN auxin efflux carrier protein on the plasma membrane of cells involved in the polar auxin transport stream (PATS; Domagalska and Leyser, 2011). Consistent with this, the Arabidopsis branching *max* mutants show increased polar PIN accumulation and increased auxin transport (Bennett et al., 2006; Prusinkiewicz et al., 2009; Crawford et al., 2010). The rice SL-deficient *d27* mutant also shows increased auxin transport (Lin et al., 2009), but this difference is not always observed in pea (Beveridge, 2000, 2006; Beveridge et al., 2000; Dun et al., 2006). In the auxin transport model, the auxin exported from active apices, moving in the PATS, would prevent auxin export from dormant buds and, therefore, would block their outgrowth, this process being amplified by the canalization positive feedback. Buds would compete to export auxin into the main stem, and SL, by dampening auxin transport in the PATS, would enhance this competition (Crawford et al., 2010; Domagalska and Leyser, 2011).

How SL and CK interact to control axillary bud outgrowth is still not understood, and the role of auxin is still a matter of debate. However, the discovery of SL as a plant hormone allows novel approaches. In particular, the discovery of genes responding to SL application and deciphering SL signaling pathways are essential for a better understanding of the control of branching. Axillary buds have to integrate many factors that influence switching between dormant and growing states during plant ontogeny, and they can respond differently according to their position along the main stem (Cline, 1991). It is very likely that several pathways control axillary bud outgrowth and that important molecular processes within the bud are involved in this control, in particular to integrate the multiple long-distance signals. In this paper, *PsBRC1*, the pea homolog of *TEOSINTE BRANCHED1* (*TB1*) from maize (*Zea mays*; Doebley et al., 1997) and of *BRANCHED1* (*AtBRC1*) from Arabidopsis (Aguilar-Martínez et al., 2007; Finlayson, 2007), was integrated into the pea model. This gene is almost exclusively expressed in the axillary bud and may provide the link between systemic signaling and events occurring within the axillary bud to control bud outgrowth.

Table I. *Summary of the physiological characteristics of the different pea branching mutants*

RMS1 expression indicates *RMS1* mRNA accumulation in epicotyl, and Response to GR24 indicates the inhibition effect of GR24 on bud outgrowth.

Characteristic	*rms1*	*rms5*	*rms3*	*rms4*	*rms2*	*Psbrc1*
RMS1 expression	High	High	High	High	Low	Low
Response to GR24	Yes	Yes	No	No	Yes	No
X-CK	Low	Low	Low	Low	High	Wild type/high
Plant height	Dwarf	Dwarf	Dwarf	Dwarf	Dwarf	Near wild type

The *TB1* gene from maize, which affects plant and inflorescence architecture, is a well-known target for artificial selection during maize domestication from its wild and highly branched ancestor teosinte (*Zea mays* ssp. *parviglumis*). It is a striking example of how human selection modified gene expression to change plant architecture. In maize, the repression of branching results from higher *TB1* transcript levels in axillary buds in comparison with those in teosinte (Doebley et al., 1997; Wang et al., 1999). Recently, it has been demonstrated that the corresponding gene in barley (*Hordeum vulgare*; *INTERMEDIUM-C*) has also been targeted in human selection to regulate not only tillering but also fertility of the lateral spikelet (Ramsay et al., 2011). In monocots, only one homolog of the TB1/CYCLOIDEA (CYC) clade has been identified that regulates axillary bud outgrowth, whereas in Arabidopsis, two homologs (*AtBRC1* and *AtBRC2*) were shown to control shoot branching. These genes belong to the TCP family of transcription factors specific to plants and named for the first three identified members, TB1, CYC in *Antirrhinum majus*, and PCF-coding genes in rice. Phylogenetic analysis of this family comprising 24 members in Arabidopsis (Martín-Trillo and Cubas, 2010) has identified two distinct classes, classes I and II, with roles in plant development and morphogenesis processes as diverse as the establishment of floral symmetry, plant architecture (Doebley et al., 1997; Aguilar-Martínez et al., 2007), leaf morphogenesis (Nath et al., 2003; Palatnik et al., 2003; Ori et al., 2007) and senescence (Schommer et al., 2008), embryo growth (Tatematsu et al., 2008), and circadian rhythm (Pruneda-Paz et al., 2009; Giraud et al., 2010). Globally, class I TCP proteins appear to promote cell division, whereas class II proteins, containing TB1/AtBRC1, repress organ growth by inhibiting cell proliferation (Martín-Trillo and Cubas, 2010). For example, class I TCP proteins, PCF1 and PCF2, were shown to promote *Proliferating Cell Nuclear Antigen* (*PCNA*) gene expression, activating the G1-to-S transition by binding to cis-acting elements in the promoter of *PCNA* (Kosugi and Ohashi, 1997). Class II TCP proteins, CINCINNATA in *Antirrhinum* and TCP4 in Arabidopsis, control leaf morphology by repressing cell proliferation specifically in the leaf margins (Nath et al., 2003; Palatnik et al., 2003; Crawford et al., 2004). In yeast, TCP4 has been shown to function in a dose-dependent manner and to block the cell cycle at the G1-to-S transition (Aggarwal et al., 2011).

In rice, the high-tillering *fine culm1* (*fc1*) mutant is mutated in the rice homolog of *TB1* (Takeda et al., 2003; Arite et al., 2007). Both the absence of response of the *fc1* mutant to GR24 application and the similarity of the phenotype of the *fc1 d17* double mutant to the SL-deficient *d17* mutant phenotype suggested that *FC1/OsTB1* acts downstream of the SL pathway in rice (Minakuchi et al., 2010). Here, we show that the regulation of pea *PsBRC1* exhibits several similarities to and differences from those described in rice and Arabidopsis. *PsBRC1* is strongly transcriptionally up-regulated by SL, which is not the case for the rice *FC1* (Minakuchi et al., 2010). In contrast to Arabidopsis (Aguilar-Martínez et al., 2007), branching is increased in the pea *Psbrc1* mutant in response to decapitation and to CK application. We propose that *PsBRC1*, acting in axillary buds, may integrate at the transcriptional level the SL and CK pathways to regulate axillary bud outgrowth. However, the response to decapitation and to direct CK application of the *Psbrc1* mutant also suggests a *PsBRC1*-independent component of the CK response in pea.

RESULTS

The Pea *Psbrc1* Mutant Phenotype Shows That *PsBRC1* Inhibits Bud Outgrowth

To isolate a pea homolog of *TB1/AtBRC1*, the sequence of the *Lotus japonicus CYC5* gene, *LjCYC5* (GenBank accession no. DQ202478; Feng et al., 2006) was used, as it was the closest homolog to Arabidopsis *TCP18/AtBRC1*. A 400-bp pea homolog sequence was first amplified with degenerate primers. The complete sequence was obtained using PCR walking and RACE PCR (GenBank accession no. JF274232, BankIt1431647; see "Materials and Methods").

Phylogenetic analysis based on the protein sequences of the TCP domain of several members of both the *CYC-TB1* group and the PCF group placed the pea sequence in the same clade as *TB1* and *AtBRC1*; consequently, the gene was named *PsBRC1* (Supplemental Fig. S1). The single intron in *PsBRC1* deduced from alignment of the genomic and cDNA sequences was located at the site of the last intron in *AtBRC1* (data not shown). *PsBRC1* was then mapped using the recombinant inbred line population (Térèse × Torsdag; Laucou et al., 1998) to the pea linkage group IV close to *Fa* in a region where no *RMS* genes were ever mapped (Rameau et al., 1998). Consequently, a targeting-induced local lesions in genomes (TILLING) approach was initiated using the mutagenized population from the genotype Caméor (Triques et al., 2007; Dalmais et al., 2008). The genomic sequence comprising the two conserved TCP and R domains was screened for mutations (Fig. 1A). Ten mutations in *PsBRC1* were identified, three giving a silent mutation, one in the intron, and six leading to a change of amino acid (Supplemental Table S1). Among these six mutations, only one gave a clear branching phenotype cosegregating with the mutation (family 4654). In all segregating populations, this mutation always cosegregated with a strong branching phenotype as in the BC2-F2 population (4654 × Caméor), where the 14 *Psbrc1* mutant plants displayed a thin stem with a strong branching phenotype at nodes 1 and 2, in contrast to the nine wild-type plants, which had a small branch only at node 2 (Supplemental Fig. S2A). This mutation was located in the TCP domain and resulted from a Thr-to-Ile amino acid change in the loop/helix II transition (T195I).

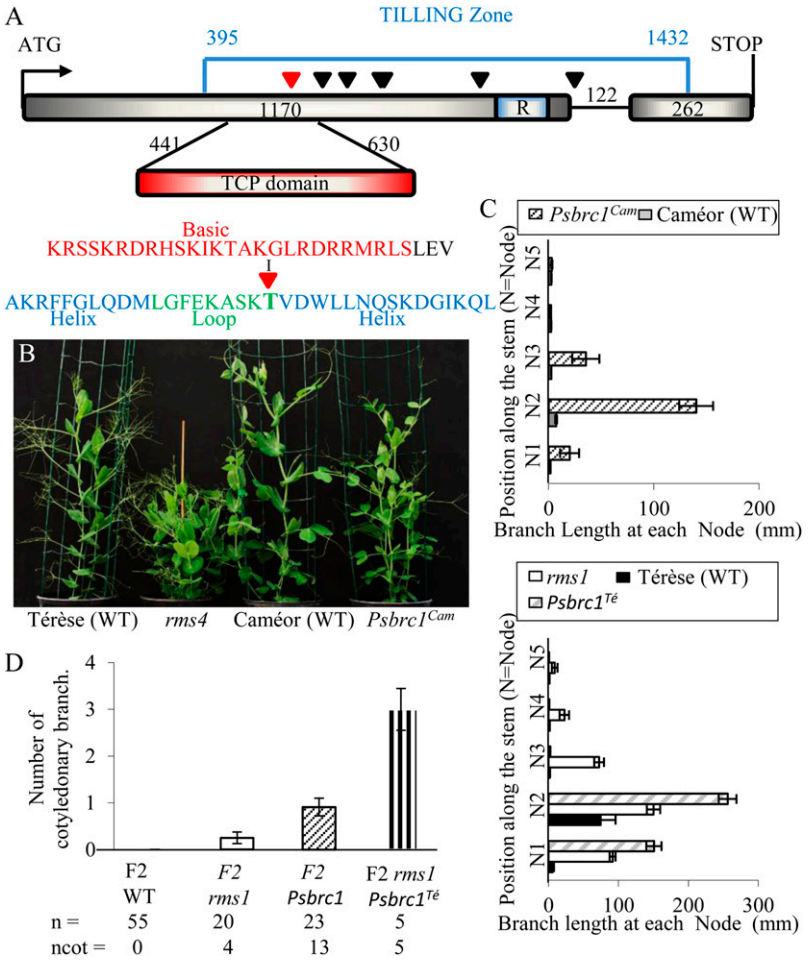

Figure 1. Structure of the *PsBRC1* gene and phenotype of the corresponding mutant. A, Gene structure of *PsBRC1* and locations of mutations. Bases are numbered from the start codon. The TCP domain (from bp 441 to 630) is shown in red, and the corresponding protein sequence is indicated below. Point mutations are indicated by triangles (black and red for the one studied here), boxes correspond to exons, and the blue area corresponds to the TILLed sequence. B, Comparison of a wild-type (WT) Térèse plant (left) with *rms4* (middle left), wild-type Caméor (middle right), and *Psbrc1*^{Cam} (right). C, Branch length at each node of wild-type Caméor, *Psbrc1*^{Cam}, wild-type Térèse, *rms1*, and *Psbrc1*^{Te}. Data are means ± SE (n = 12). D, Means of the number of cotyledonary branches per individual observed in a segregating F2 population of 103 plants between M3T-884 (*rms1*) and a *Psbrc1* F2 plant (*Psbrc1*^{Cam} × Térèse). n = the number of plants observed per genotypic class; ncot = the number of plants with at least one cotyledonary branch. Data are means ± SE (n = 12).

These data strongly support the hypothesis that the T195I mutation in the *PsBRC1* gene was the cause of the high-branching phenotype.

The mutant plant from family 4654 was backcrossed three times with the Caméor parent line (BC3 [4654 × Caméor]; denoted *Psbrc1*^{Cam}) and twice with the wild-type Térèse line in which all other branching mutations are available (mutant line denoted *Psbrc1*^{Te}; see "Materials and Methods"). The phenotype of *Psbrc1*^{Cam} was first compared with its wild-type progenitor Caméor. Strong basal branching at nodes 1 and 2 was observed in the *Psbrc1*^{Cam} mutant, with often two branches at node 2, whereas the wild-type Caméor sometimes showed only a single branch at node 2. Branching at upper nodes (above node 3) was very low in *Psbrc1*^{Cam} (Fig. 1, B and C, top diagram). The low branching at upper nodes observed in *Psbrc1*^{Cam} was particularly evident in the *Psbrc1*^{Te} mutant and was one major difference from the *rms1* mutant, which showed, in comparison, long branches at each node (Fig. 1C, bottom diagram; Supplemental Fig. S2D). Another difference between the mutants was that plant height was only slightly reduced for *Psbrc1*^{Cam} and *Psbrc1*^{Te} in comparison with their respective wild types, whereas *rms1* showed a strong reduction in internode length (Fig. 1B; Supplemental Fig. S2B). The width of the main stem was reduced in both *rms1* and *Psbrc1*^{Cam} mutants (Supplemental Fig. S2C).

rms1 Psbrc1 double mutant plants were obtained from a cross between the *rms1* mutant derived from the wild-type Térèse (line M3T-884) and a *Psbrc1* F2 plant derived from the cross Térèse × *Psbrc1*^{Cam}, also containing the *afila* mutation (absence of leaflets as in the wild-type Térèse). In the F2 generation, 103 plants were genotyped for both genes and phenotyped. A striking feature of double mutant plants was the high number of cotyledonary branches per plant. In this particular genetic background, approximately half of the *Psbrc1* plant displayed cotyledonary branches, which is rarely seen for *Psbrc1*^{Cam} in the Caméor genetic background, whereas only four out of 20 *rms1* plants (that were all heterozygous for *PsBRC1*) branched at this cotyledonary node (Fig. 1D). A more precise phenotyping was performed on five or six F3 families fixed for *rms1*, *Psbrc1*, or both mutations in a comparable genetic background (see "Materials and Methods"). As observed previously, at upper nodes, *rms1* plants were significantly more branched than *Psbrc1*^{Te} plants, whereas the double mutant genotype was not significantly more branched than *rms1* at these

nodes (Supplemental Fig. S2D; $P < 0.05$ by LSD test). At node 2, total branch length was similar in the three genotypes, whereas at nodes below, and particularly at the cotyledonary node, branching of *rms1 Psbrc1* double mutant plants was significantly higher than in either single mutant (Supplemental Fig. S2D). Consequently, it appeared that at basal nodes, a transgressive phenotype was observed in the double mutant, whereas at upper nodes, branching of the double mutant was not significantly different from that observed for *rms1*.

PsBRC1 Is a Target in the SL Signaling Pathway

To test whether *PsBRC1* was expressed mainly in axillary buds, as shown in maize, Arabidopsis, rice, and tomato (*Solanum lycopersicum*; Hubbard et al., 2002; Takeda et al., 2003; Aguilar-Martínez et al., 2007; Martin-Trillo et al., 2011), wild-type plants were dissected into different organs/parts and *PsBRC1* transcript levels were quantified by real-time PCR. Transcripts were only detected in axillary buds, floral buds, nodal tissue, and the shoot apex. Maximum transcript levels were found in axillary buds. Floral buds, shoot apex, and nodal tissue contained very low levels of transcripts, 100 to 1,000 times less than in axillary buds (Supplemental Table S2).

The response of the *Psbrc1*^{Cam} mutant to SL was analyzed by application of the synthetic SL GR24 (500 nM) to the axillary bud at node 3 of both *Psbrc1*^{Cam} and *rms1* mutants and their respective wild types. Bud length was measured 10 d later (Fig. 2A). No inhibitory effect of GR24 was observed for the wild-type Térèse and Caméor, in which axillary buds are very small at this node. In contrast to the strong inhibition of axillary bud outgrowth in the SL-deficient *rms1* mutant, no significant effect of GR24 was observed for the *Psbrc1*^{Cam} mutant (Student's *t* test, $P = 0.89$). Grafting experiments confirmed the SL insensitivity of *Psbrc1*^{Cam}, as branching was not inhibited when the *Psbrc1*^{Cam} mutant scion was grafted on wild-type rootstock, in contrast to the SL-deficient *rms1* scion grafted on wild-type rootstock (Supplemental Fig. S3). *Psbrc1*^{Cam} rootstocks were able to inhibit branching in the *rms1* scion, indicating that *Psbrc1*^{Cam} very likely produces SL and/or the active derived compound (Supplemental Fig. S3). To confirm that *Psbrc1*^{Cam} was able to synthesize SL, we quantified SL in root exudates of *Psbrc1*^{Cam}, *Psbrc1*^{Te}, and their corresponding wild types (Fig. 2B). The principal SL detected in root exudates of all genotypes was fabacyl acetate. Amounts of this compound were 3- to 6-fold higher ($P < 0.05$, Student's *t* test) from both *Psbrc1* genotypes than in their corresponding wild-type background lines (Fig. 2B). Other compounds, particularly epiorobanchyl acetate, were detected in most samples, but levels were too low for accurate quantitation.

The *PsBRC1* transcript level was quantified in axillary buds of the different SL-related mutants using

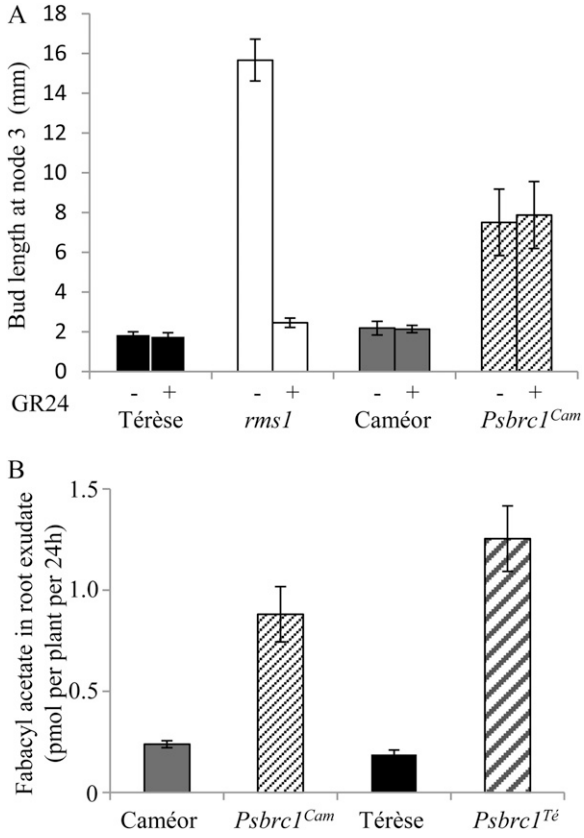

Figure 2. A, Effects of GR24 application on bud growth. Bud length at node 3 of wild-type Térèse (black bars), *rms1* (white bars), wild-type Caméor (gray bars), and *Psbrc1*^{Cam} (hatched bars) was measured 10 d after treatment was applied to buds of stage 5 intact plants with solution containing 0 or 500 nM GR24. Data are means ± SE ($n = 12$). B, SL levels in root exudates of wild-type and *Psbrc1* plants. Exudates were collected into water for 24 h from 20-d-old hydroponically grown plants, and SLs were quantified by LC-MS using MRM transitions at mass-to-charge ratio 405 to 231 for fabacyl acetate and 406 to 232 for the d_1-fabacyl acetate internal standard. Data are means ± SE, based on analyses of two independent pools of 12 plants for each genotype.

real-time PCR (Fig. 3A). Dissected axillary buds were sampled from node 4 of the *rms1*, *rms2*, and *rms4* mutants and the wild-type line (Térèse) at a stage when buds had a comparable size (before they start to grow in mutants). *PsBRC1* levels were 10 times lower in *rms1* and *rms4* than in the wild type (Fig. 3A; Supplemental Fig. S4, A and B). These results indicated that *PsBRC1* may act downstream of the SL signaling pathway and downstream of *RMS4*. In contrast, the *PsBRC1* transcript level was similar to the wild-type level in axillary buds of the *rms2* mutant (Fig. 3A). The *rms2* mutant displays strong basal branching in comparison with *rms1* (Dun et al., 2009), and at node 4, from where the buds were sampled, the axillary buds of *rms2* plants were only 2.3 mm long, whereas they reached 14 mm in *rms1* (data not shown). The *rms2* phenotype of inhibited

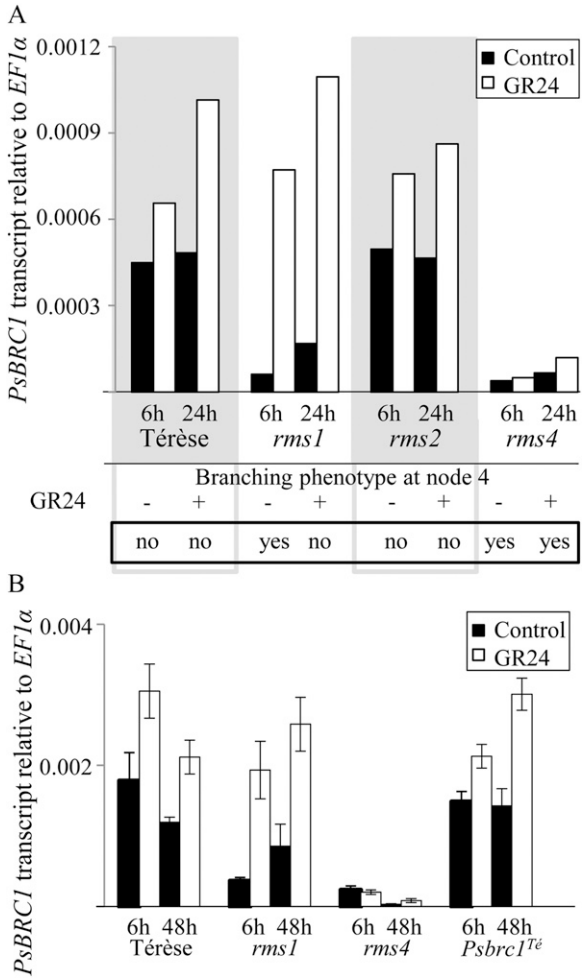

Figure 3. Effects of GR24 on *PsBRC1* transcript levels. *PsBRC1* transcript levels were determined relative to EF1α in axillary buds at node 4 after GR24 application (white bars) or mock treatment (black bars). RNA was extracted from dissected buds from pools of 30 plants at the six-node stage and quantified by real-time PCR. The data are representative of two to three independent experiments. A, Six and 24 h after GR24 application in wild-type Térèse, *rms1*, *rms2*, and *rms4* plants. The branching phenotype at node 4 after GR24 application is given below for each genotype. B, Six and 48 h after GR24 application in wild-type Térèse, *rms1*, *rms4*, and *Psbrc1*^{Té} plants. Data are means ± SE (n = 3).

buds at node 4 is explained by a (basal) branch-derived feedback signal, possibly auxin, which increases *RMS1* expression and presumably SL synthesis in *rms2* plants (Dun et al., 2009). This SL moves up the stem and, because the *rms2* mutant is able to synthesize and to respond to SL, it could explain why in this branching mutant *PsBRC1* transcript levels were not low at this upper node.

To further characterize the relationship between SL and *PsBRC1* expression, *PsBRC1* transcript levels were followed from 6 h up to 24 h after SL application (Fig. 3A). Transcript levels increased in axillary buds of wild-type, *rms1*, and *rms2* plants after GR24 application (500 nM) but not in *rms4* (Fig. 3A; Supplemental Fig. S4A). In wild-type and *rms2* axillary buds, a 2-fold increase was observed 24 h after GR24 application. In *rms1* mutant buds, *PsBRC1* mRNA levels increased 10-fold at 6 and 24 h after GR24 treatment (Fig. 3A; Supplemental Fig. S4A). In *rms4*, there was no effect of GR24 treatment, with *PsBRC1* transcript levels remaining very low throughout (Fig. 3A; Supplemental Fig. S4A). To test if the induction of *PsBRC1* by GR24 is affected in *Psbrc1*, the *Psbrc1*^{Te} mutant was included in one experiment with the wild-type Térèse, *rms1*, and *rms4*. *PsBRC1* transcript levels were followed from 6 to 48 h after GR24 application (Fig. 3B). *PsBRC1* transcript levels were very low in *rms1* and *rms4* axillary buds compared with wild-type and *Psbrc1*^{Te} axillary buds. In several experiments, transcript levels of *PsBRC1* were not reduced in the *Psbrc1*^{Cam} mutant in comparison with levels in the corresponding wild-type Caméor (Figs. 3B and 4A; Supplemental Fig. S4B), whereas they were reduced in SL-deficient and SL-response mutants. Again, *PsBRC1* transcript levels remained very low in *rms4*, whereas a strong increase was observed after GR24 treatment in *rms1*. In the wild type and the *Psbrc1*^{Te} mutant, a 2-fold increase of *PsBRC1* by GR24 was generally observed, in contrast to the noninduction in the *rms4* background (Fig. 3B). All these results indicate that *PsBRC1* transcription and its induction by GR24 are not affected in the *Psbrc1* mutant.

CK Regulates *PsBRC1* at the Transcriptional Level Independently of SL

To investigate whether CK regulates the transcription of *PsBRC1*, axillary buds at node 4 of *Psbrc1*^{Cam}, *rms1*, and *rms4* mutants and their corresponding wild types were harvested 6 h after direct application of the synthetic CK 6-benzylaminopurine (BAP; 50 μM), and *PsBRC1* transcript levels were quantified using real-time PCR (Fig. 4A; Supplemental Fig. S4B). In all genotypes, BAP application led to a strong reduction of *PsBRC1* transcript levels. This included the *rms1* SL-deficient and the *rms4* SL-response mutants, in which *PsBRC1* transcript levels were already low. The CK effect on *PsBRC1* expression in *rms4* buds shows that CK can transcriptionally regulate *PsBRC1* independently of SL.

The *Psbrc1*^{Cam} Mutant Responds to Exogenous CK Application and to Decapitation

To test whether *PsBRC1* is needed for axillary bud growth, CK was applied to bud 4 of wild-type Térèse and Caméor and *rms4* and *Psbrc1*^{Cam} mutants and buds were measured 5 and 7 d after application (Fig. 4B). For all lines, axillary buds did not grow much without CK treatment, as in this experiment, to have a better comparison between wild-type and mutants, the primary bud at upper nodes in mutants was removed prior to the treatment, as were the basal lateral

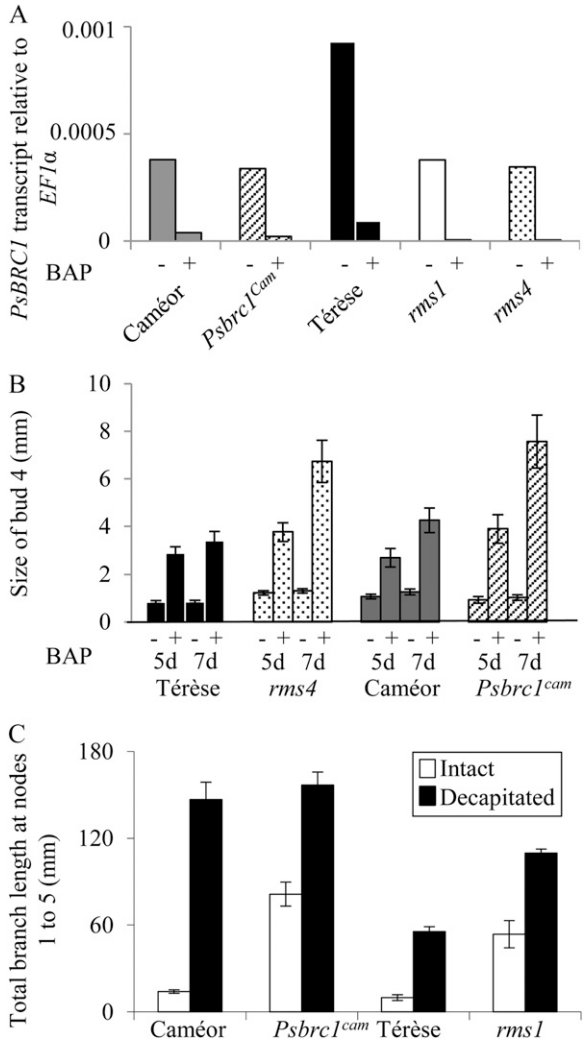

Figure 4. Effects of BAP on *PsBRC1* transcript levels and on bud growth. A, *PsBRC1* transcript levels were determined relative to *EF1α* in axillary buds at node 4 after BAP (50 μM) application in wild-type Caméor, *Psbrc1*^{Cam}, wild-type Térèse, *rms1*, and *rms4*. RNA was extracted from the dissected buds of 30 plants at the six-node stage and quantified by real-time PCR. The data are representative of three independent experiments. B, Effects of BAP (50 μM) treatment on bud growth at node 4 in wild-type Térèse, *rms4*, wild-type Caméor, and *Psbrc1*^{Cam}. Measurements were done 5 d after treatment. Data are means ± SE (n = 12). C, Effects of decapitation above node 5 on total branch length at nodes 1 to 5. Intact and decapitated plants of *Psbrc1*^{Cam}, wild-type Caméor, *rms1*, and wild-type Térèse were used. Data are means ± SE (n = 8).

branches for all genotypes. All genotypes responded to BAP application by displaying a strong increase in bud/branch length compared with the mock-treated buds, particularly for *rms4* and *Psbrc1*^{Cam} mutants. Another way to test the response to CK is decapitation, which, by depleting the source of auxin, has been shown to induce a rapid and massive decrease of *RMS1* SL biosynthesis gene expression, together with rapid increases in CK level in xylem sap and in transcript levels of CK biosynthesis genes in nodal tissue (Bangerth, 1994; Foo et al., 2005; Tanaka et al., 2006; Foo et al., 2007). Decapitation of *rms1* and *Psbrc1*^{Cam} mutants and their corresponding wild types resulted in increased branch lengths in all genotypes (Fig. 4C). Because the *Psbrc1*^{Cam} mutant has been shown to be insensitive to GR24 application, its response to decapitation suggests that this response may be largely due to CK level variation occurring after decapitation or to CK-independent effects of auxin depletion.

PsBRC1 and the *RMS2*-Dependent Feedback Signal

The SL biosynthesis gene *RMS1/CCD8* is highly regulated at the transcriptional level. In particular, the absence of SL response because of SL deficiency (in *rms1* and *rms5*) or the lack of response (in *rms3* and *rms4*) induces a feedback signal that strongly up-regulates *RMS1* transcript levels (Beveridge et al., 1997a, 1997b; Beveridge, 2000; Foo et al., 2005). The *RMS2* gene may control this feedback signal, as *RMS1* transcript levels are not up-regulated in the *rms2* mutant. *RMS1* transcript accumulation was quantified in epicotyls from *rms1*, *rms2*, *rms4*, and *Psbrc1*^{Cam} mutants and their corresponding wild types (Fig. 5A; Supplemental Fig. S4E).

Consistent with previous findings, *RMS1* mRNA was more abundant in *rms1* and especially in *rms4* mutants compared with wild-type Térèse. In contrast, *rms2* and *Psbrc1*^{Cam} mutants contained three and six times lower transcript levels compared with their respective wild-type lines, suggesting that the feedback signal is not activated in the *Psbrc1* background. As the same feedback signal appears to control X-CK (Beveridge et al., 1997a; Beveridge, 2000; Foo et al., 2005, 2007), X-CK of wild-type and *Psbrc1*^{Cam} plants was measured in two separate experiments (Fig. 5B). The main compounds detected were trans-zeatin riboside and dihydrozeatin riboside. Smaller amounts of isopentenyl adenosine, trans-zeatin, cis-zeatin riboside, isopentenyl adenine, and dihydrozeatin were also present. The profiles of CKs and absolute amounts were very similar in both experiments, with no statistically significant differences between wild-type and *Psbrc1*^{Cam} genotypes (Student's t test, P = 0.49). This contrasts with Arabidopsis *max* and pea *rms* branching mutants, which, with the exception of *rms2*, have highly depleted X-CK levels (Table I; Beveridge et al., 1997a; Foo et al., 2007). Levels of X-CK were also quantified in *rms1 Psbrc1* double mutant plants in comparison with wild-type and single mutant plants derived from the same cross, to have a comparable genetic background and to have enough plants for sap collection (see "Materials and Methods"). X-CK levels in the F3 *rms1 Psbrc1* double mutant plants were not significantly different from X-CK levels from F3 *rms1* plants, whereas X-CK levels from F3 *Psbrc1* and *Psbrc1*^{Te} were particularly high in comparison with wild-type Térèse and F3 wild-type plants. The greatly

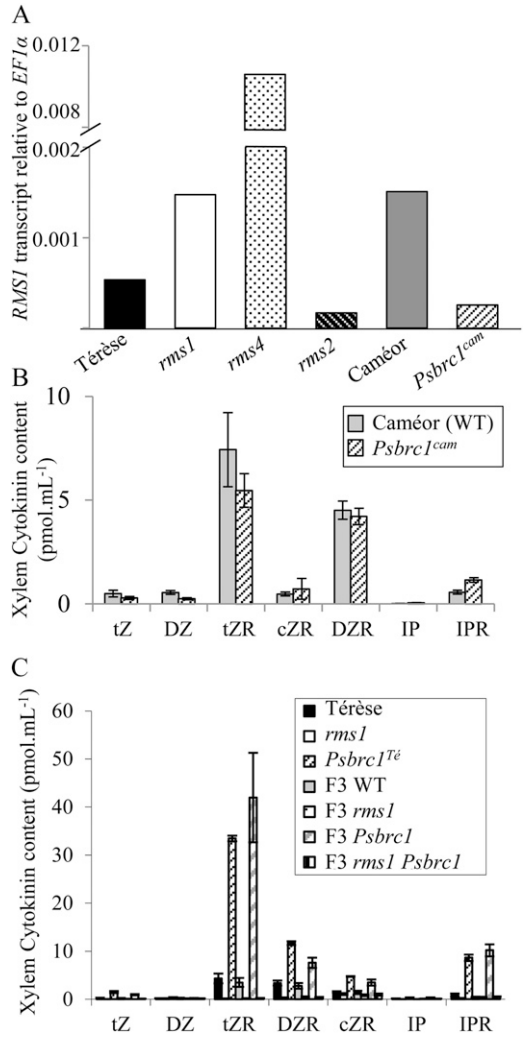

Figure 5. The *RMS2*-dependent feedback signal is not activated in *Psbrc1*. A, *RMS1* transcript levels were determined in epicotyls of *rms1*, *rms2*, *rms4*, and their corresponding wild-type Térèse as well as *Psbrc1*^{Cam} and its corresponding wild-type Caméor. RNA was extracted from plants at stage 6. The data are representative of three independent experiments. B and C, CK contents of root xylem sap. tZ, trans-Zeatin; DZ, dihydrozeatin; tZR, trans-zeatin riboside; DZR, dihydrozeatin riboside; cZR, cis-zeatin riboside; IP, isopentenyl adenine; IPR, isopentenyl adenosine. B, Wild-type (WT) Caméor and the *Psbrc1*^{Cam} mutant. C, Wild-type Térèse, M3T-884 (*rms1*), *Psbrc1*^{Té}, and F3 plants with wild-type, *rms1*, *Psbrc1*, and *rms1 Psbrc1* genotypes derived from four F2 (M3T-884 × F2 [Térèse × *Psbrc1*^{Cam}]) populations (see "Materials and Methods"). Measurements were made from pools of 3 mL of sap harvested from 20 to 40 plants. Data are means ± SE (n = 3).

increased X-CK in *Psbrc1*^{Te} in this experiment was not seen in the previous analysis with *Psbrc1*^{Cam} and its wild-type Caméor and may relate to genetic background. Overall, these results indicate that the feedback regulation of X-CK is restored in the *Psbrc1 rms1* double mutant but is absent or misregulated in *Psbrc1* single mutants.

DISCUSSION

The Phenotype of *Psbrc1* Differs from the Phenotype of the SL-Deficient *rms1* Mutant

Despite its large genome and recalcitrance to transformation, pea is an excellent model plant for genetic and physiological studies. The TILLING approach is particularly adapted for reverse genetics in such model plants (Triques et al., 2007; Dalmais et al., 2008) and has been applied in this work to identify a novel branching mutant in the TCP transcription factor *PsBRC1*. The *Psbrc1* mutant showed a strong branching phenotype in comparison with its wild-type progenitor Caméor, particularly at basal nodes; buds at upper nodes were larger or gave small branches in comparison with the wild-type. When compared with the SL-deficient *rms1* mutant, the *Psbrc1* mutant displayed very few long branches at upper nodes. Moreover, its height was less affected compared with *rms1* and other *rms* mutants, which are relatively dwarf. In rice, the *fc1* mutant is also less affected in height and in tiller number than the *dwarf* (*d*) SL mutants (Arite et al., 2007). In tomato, the phenotype of *SlBRC1b* RNA interference lines is also less strong than the phenotype of the *Slccd7* lines (Martin-Trillo et al., 2011), which supports the idea that the milder phenotype of *Psbrc1* compared with *rms1* is likely not due to a leaky mutation. In addition, the Thr mutated to Ile in the studied *Psbrc1* pea mutant (T195I) is located in the loop/helix II transition and appears highly conserved in the class I TCP family and in the class II CYC/TB1 clade (Martín-Trillo and Cubas, 2010). The relatively mild branching phenotype could also explain why the intensive screenings for high-branching mutants in pea ethyl methanesulfonate-mutagenized populations previously failed to identify the *Psbrc1* pea branching mutant.

The difference of phenotypes between the SL-deficient *rms1* and *Psbrc1* mutants may be explained by the very localized expression of the *PsBRC1* gene, mostly expressed in axillary buds, in contrast to the SL biosynthesis *RMS1* and *RMS5* genes, which are highly expressed in roots and also significantly in stems, where they are regulated by different long-distance signals. Novel roles for SL in plant architecture, other than shoot branching, have been recently suggested for dwarfism (Lin et al., 2009) and root architecture (Koltai et al., 2009; Kapulnik et al., 2011; Ruyter-Spira et al., 2011). The relative dwarfism of *rms* mutants (in rice, the SL mutants were originally called *dwarf*) is not yet understood, but it is very likely that SL controls stem growth, and this control may be independent of *PsBRC1*. In the auxin transport theory, it is proposed that SL modulates polar auxin transport (PAT) in the stem and that axillary buds compete for exporting auxin into the PAT stream in the main stem. The *Psbrc1* mutant appears less branched at upper nodes than the SL-deficient *rms1* mutant, which could suggest that competition between buds is higher in the *Psbrc1*

mutant compared with the other *rms* mutants. In pea, differences in auxin transport between SL-related mutants and the wild type are modest (Beveridge et al., 2000), in contrast to Arabidopsis. It would be interesting to test if the Arabidopsis *Atbrc1* mutant has increased auxin transport, as observed in *max* mutants (Bennett and Leyser, 2006), as this would reveal whether the relative pleiotropy of the SL-deficient and SL-response mutants in comparison with *Atbrc1* is related to a difference in PAT. In Arabidopsis, two *TB1* homologs have been identified, *AtBRC1* and *AtBRC2*, with a role in the control of shoot branching (Aguilar-Martínez et al., 2007). The presence of a second *BRC1* homolog in pea and gene redundancy could also explain the weaker phenotype of *Psbrc1* in comparison with the SL mutants. Nevertheless, we were unable to amplify another pea *BRC* homolog, and in Arabidopsis, the double *Atbrc1 Atbrc2* mutant displays the same branching phenotype as the strongest *Atbrc1* mutant (Aguilar-Martínez et al., 2007).

PsBRC1 Acts Downstream of the SL Pathways to Control Axillary Bud Outgrowth

The fact that the *Psbrc1* mutant did not respond to SL application suggests that *PsBRC1* may be involved in the SL signaling pathway to repress axillary bud outgrowth. In support of *BRC1* acting in the SL pathway, we showed that *PsBRC1* expression in axillary buds was rapidly enhanced by SL treatment. *PsBRC1* transcript levels were very low in axillary buds of SL-deficient (*rms1*) or SL-response (*rms4*) mutants in comparison with wild-type buds but were rapidly up-regulated by SL application, particularly in *rms1*, in which it was already very low, and in the wild type, *rms2*, and *Psbrc1*. As expected for a SL-response mutant, *PsBRC1* transcript levels remained very low after SL treatment in buds of the *rms4* response mutant. Although RMS4 has not been proven to act in the SL pathway, it has all the features expected of a protein involved in SL signaling (branching phenotype of *rms4*, F-box protein, nonresponse to GR24 application of the *rms4* mutant, strong feedback up-regulating *RMS1* expression in the *rms4* mutant). As such, the *RMS4*-dependent response of *PsBRC1* to SL is consistent with *PsBRC1* acting in the SL signaling pathway for branching inhibition. The expression of *PsBRC1* in the *Psbrc1* mutant was similar to its expression in the wild type, and the increase of *PsBRC1* expression after GR24 application was not affected in the *Psbrc1* mutant, despite the fact that the branching of this mutant was not repressed by GR24 application. These data indicate that *PsBRC1* transcript levels do not simply correlate negatively with the activity of axillary buds and suggest a direct effect of the *PsBRC1* transcription factor in the repression of axillary bud outgrowth. In rice, the homolog of the maize *TB1* gene, *FC1*, was found not to be transcriptionally up-regulated by SL (Minakuchi et al., 2010). In Arabidopsis, expression of *AtBRC1* was strongly down-regulated in the *max1* to *max4* mutants (Aguilar-Martínez et al., 2007), suggesting that SL up-regulates transcript levels of *AtBRC1* in Arabidopsis, as we observed for *PsBRC1*. In contrast, the other homolog, *AtBRC2*, is not down-regulated in the *max1* and *max2* mutants; *FC1* and *AtBRC2* appear to be similarly unresponsive to SL, while *AtBRC1* and *PsBRC1* are both transcriptionally up-regulated by SL.

To confirm that *PsBRC1* and *RMS1* act in the same pathway, *rms1 Psbrc1* double mutant plants were produced and their phenotype analyzed alongside the single mutant plants in a comparable genetic background. In Arabidopsis and rice, the corresponding double mutants have the same level of branching as single mutants (Aguilar-Martínez et al., 2007), suggesting that the FC1/AtBRC1 TCP transcription factors act in the SL pathway. In pea, surprisingly, total branch length was strongly enhanced in the *rms1 Psbrc1* double mutant plants, mainly because of strong development of the cotyledonary branches. When branching was quantified according to the position along the stem, branching of *rms1 Psbrc1* was similar to branching in *rms1* at upper nodes (node 3 and above) but transgressive at basal nodes (cotyledonary node and node 1). These results suggest a possible specific regulation of branching at basal nodes in pea. Unlike in Arabidopsis, these buds are differentiated very early in the embryo at the axils of particular leaves (cotyledons and scale leaves) and their development generally occurs below the soil surface. In pea, the *RMS6* gene has been shown to control bud outgrowth only at these nodes (Rameau et al., 2002). Future studies will have to decipher how branching is regulated at these basal nodes and how *RMS6*, SL, and *PsBRC1* interact to have a better understanding of the phenotype of the *rms1 Psbrc1* double mutant.

CK Regulates Bud Outgrowth via *PsBRC1* and Sustained Bud Growth Independently of *PsBRC1*

Our results showed that *PsBRC1* transcript levels decrease after direct application of CK to the axillary bud for all genotypes tested, including the SL-response *rms4* and *Psbrc1* mutants. These results demonstrate that CK controls *PsBRC1* expression independently of the SL pathway. Thus, *PsBRC1* could integrate the SL and CK pathways at the transcriptional level within the bud and bud outgrowth would occur where *PsBRC1* falls below a certain transcript level. In rice, similar results have been obtained, with a strong decrease of *FC1* expression 3 h after BAP treatment (Minakuchi et al., 2010).

We tested the phenotypic response of CK application on axillary buds at node 4 of $Psbrc1^{Cam}$, *rms4*, and their corresponding wild-type progenitors. CK treatment induced bud outgrowth for all genotypes, including $Psbrc1^{Cam}$. This response indicates that CK may promote axillary bud outgrowth and/or growth independently of the SL signaling pathway and from *PsBRC1*. The phenotypic response to decapitation was consistent with the CK response of $Psbrc1^{Cam}$ and of the

SL-deficient *rms1* mutant. This result differs from that observed in Arabidopsis, where *Atbrc1* mutants showed no response to decapitation (Aguilar-Martínez et al., 2007). This difference between pea and Arabidopsis could be explained by the stage of development when the decapitation was performed (a floral shoot was decapitated in the case of Arabidopsis compared with decapitation of a vegetative shoot in pea) and by the different growth habits of these species (Cline, 1996). If *PsBRC1* integrates the SL and CK signals to control axillary bud outgrowth, the CK response of the *Psbrc1*^{Cam} mutant could be interpreted as the CK response having at least two components, one involving early bud outgrowth (*PsBRC1* dependent) and the other involving sustained growth (*PsBRC1* independent; Dun et al., 2009). Indeed, branching involves many steps, from axillary meristem initiation and axillary bud formation to axillary bud outgrowth and sustained growth of branches. Simple quantification of the lengths of buds/lateral branches does not in itself distinguish the different growth stages.

The RMS2-Dependent Feedback Signal Originates between RMS4 and PsBRC1

The existence of a mobile graft-transmissible auxin-independent shoot-to-root feedback signal that up-regulates *RMS1* and *RMS5* transcription and down-regulates X-CK export from roots was previously proposed (Beveridge et al., 2009; Dun et al., 2009). Because the *rms2* mutant showed low *RMS1* expression and high X-CK content in the xylem sap, in contrast to the other *rms* mutants (Table I), it was suggested that the shoot-to-root feedback signal was *RMS2* dependent (Beveridge et al., 2000). Experiments with grafted plants bearing two shoots of different genotypes and different phenotypes indicated that the feedback signal was more likely generated by the branching shoot to suppress X-CK and up-regulate *RMS1* expression, even in the presence of a nonbranching wild-type shoot. Moreover, experiments with mutants lacking axillary meristems in an *rms4* background demonstrated that branching per se was not the cause of the feedback (Foo et al., 2001, 2007). It was instead suggested to be regulated by the absence of perception of SL (Foo et al., 2005; Dun et al., 2009), as various mutants unable to produce (*rms1* and *rms5*) or to respond to (*rms3* and *rms4*) SL have reduced export of X-CK from the roots (Beveridge et al., 1997a; Morris et al., 2001; Foo et al., 2007) and increased expression of SL biosynthesis genes (Foo et al., 2005; Johnson et al., 2006; Arite et al., 2007; Hayward et al., 2009). Here, we showed that *Psbrc1*^{Cam} lacks the feedback up-regulation of *RMS1* gene expression and that the substantial down-regulation of X-CK content in SL biosynthesis and signaling mutants was not found in *Psbrc1*^{Cam} plants (Table I). Instead, X-CK was either nearly normal in *Psbrc1*^{Cam} or substantially increased in *Psbrc1*^{Te} mutant plants, with the response appearing to depend on genetic background in our experiments. Similarly, in rice, *D10* expression was not increased in the *fc1* mutant, whereas it was highly expressed in other SL-related mutants (Arite et al., 2007; Minakuchi et al., 2010). As discussed above, our results suggest that *PsBRC1* acts downstream of *RMS4* in the SL signaling pathway. The absence of feedback in *Psbrc1* could suggest that the SL-mediated feedback regulation is generated between the action of *RMS4* and *PsBRC1*. This is further supported by the feedback down-regulation of X-CK in *Psbrc1 rms1* double and *rms1* single mutants but not in *Psbrc1*^{Te} single mutants.

Advances in plant hormone signaling have highlighted the role of the ubiquitin-proteasome pathway and targeted protein turnover (Santner and Estelle, 2009). Because the *MAX2/RMS4* gene encodes an F-box protein (Stirnberg et al., 2002; Johnson et al., 2006), it is likely that the SL signaling pathway involves similarly targeted protein degradation. In the GA signaling pathway, DELLA proteins are repressors that act directly downstream of the GA receptor. Microarray analysis has identified early GA- and DELLA-responsive genes (Zentella et al., 2007). Among the GA-repressed and DELLA-induced targets are genes encoding GA biosynthetic enzymes, indicating the direct involvement of DELLA proteins in feedback

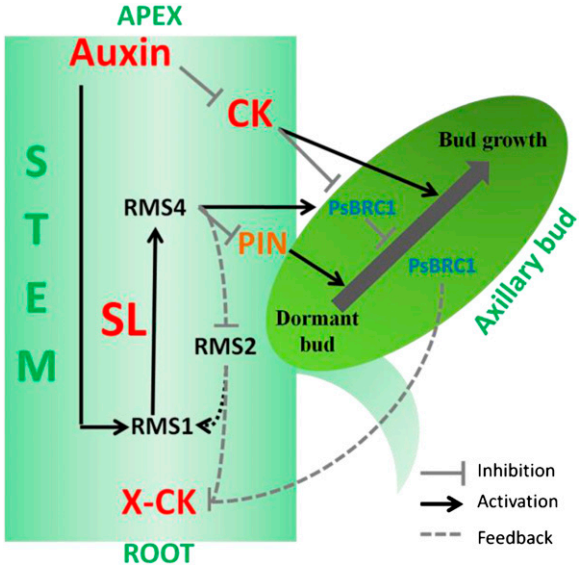

Figure 6. Model for the hormonal control of branching in pea integrating the function of *PsBRC1* in the axillary bud and the auxin transport canalization-based model (Domagalska and Leyser, 2011). *PsBRC1* integrates the SL and CK pathways to control bud outgrowth. CK also increases bud growth via a *PsBRC1*-independent pathway. Auxin maintains *RMS1* transcript levels, and hence SL synthesis, and down-regulates CK levels. The *RMS2*-dependent feedback, which up-regulates SL biosynthesis and down-regulates xylem CK, is activated when there is a lack of SL signaling via *RMS4* and may be independent of *PsBRC1*. SLs reduce PIN accumulation to the plasma membrane via *RMS4* but independently of *PsBRC1* and, by reducing the effectiveness of the canalization feedback loop, enhance the competition between active buds.

regulation. Proteins targeted for degradation in the SL signaling pathway, still to be identified, and possibly acting as repressors of *PsBRC1* may similarly regulate the feedback signal in pea controlling SL biosynthesis and X-CK.

SL quantification in root exudates of *Psbrc1* genotypes in comparison with their wild type show that this mutant is not deficient in SL biosynthesis and explains the grafting results. The higher level of fabacyl acetate found in root exudates of the two *Psbrc1* lines in comparison with their wild type, despite the low *RMS1* expression in epicotyl, is surprising and indicates a possible misregulation of SL biosynthesis in the mutant. In the rice *fc1* mutant, the level of 2′-epi-5-deoxystrigol in root exudates was slightly higher but not significantly different from the wild type (Minakuchi et al., 2010). Dun et al. (2009), using a hypothesis-driven modeling approach, suggested that SL biosynthesis is tightly regulated by multiple feedback signals in both shoot and root. More experimental data (e.g. *RMS1* expression in *Psbrc1* roots and SL quantification in shoot, xylem, and root) are needed to have a complete understanding of the signal network controlling shoot branching.

CONCLUSION

This study shows that the PsBRC1 transcription factor acts locally in the axillary bud and strongly supports that it acts downstream of SL to repress bud outgrowth. Two models are currently proposed to explain how auxin and SLs interact to control branching: the auxin transport canalization model and the second messenger model (Brewer et al., 2009; Domagalska and Leyser, 2011). The precise comparison of the *Psbrc1*^{Te} mutant phenotype with the SL synthesis (*rms1*) mutant suggests that processes within the stem may be affected in SL synthesis mutants but not in *Psbrc1*^{Te}, one of these processes being PAT. The model that best fits with our data would be one in which both regulatory systems, not mutually exclusive, as indicated previously (Domagalska and Leyser, 2011), would coexist (Fig. 6). The degree of branching of a plant is an important component of its fitness, and it is very likely that different pathways are involved in its tight control according to bud position on the stem, developmental stage, and environmental conditions. SL would act locally in axillary buds via *PsBRC1* and would also coordinate branching across the plant (Leyser, 2011) by controlling auxin transport independently of *PsBRC1*. The study of *PsBRC1* gives an example of a transcription factor with more limited phenotypic effects than its upstream signaling genes. It indicates that the SL signaling pathway may be shared among multiple developmental modules, as proposed by Doebley and Lukens (1998). Future studies will decipher these different components of SL function.

MATERIALS AND METHODS

Isolation of *PsBRC1*, Phylogenetic Analysis, and Mapping

Two degenerate primers, Cyc5F [5′-GGGA(T/C)CG(G/A)AGAATGAG (G/A)(T/C)T(G/T/C)TC-3′] and Cyc5R [5′-CTT(G/T)(T/C)TCTT(G/T)C (T/C)CTT(G/T)C(T/C)CT-3′], were designed in the conserved TCP domain of the *Lotus japonicus LjCYC5* gene. These primers were tested on pea (*Pisum sativum* 'Térèse') genomic DNA, and a fragment of 400 bp was amplified. The 5′ region was obtained with one round of 5′ RACE PCR using gene-specific nested primers 642Dn (5′-CCACTTTTTCTTGTTCTTGATTT-3′), 527Dn (5′-TGTTTGATTCCGTCTTTCG-3′), and 497Dn (5′-TAACCAGTCCACAGTTTGC-3′) followed by PCR walking with three specific primers, 497Dn, 198R (5′-GCTAGATCTTTTCCTTTGGATC-3′), and 143R (5′-GCTTCTGCAGGAACAAGAC-3′), and the restriction enzyme *Dra*I (Fermentas). The 3′ sequence of *PsBRC1* was obtained by thermal asymmetric interlaced-PCR (Liu and Whittier, 1995) with gene-specific nested primers 198F (5′-GATCCAAAGGAAAAGATCTAGC-3′) and 527Un (5′-CGAAAGACGGAATCAAACA-3′) and the RAPD primer E1 (5′-CCCAAGGTCC-3′). The amplicon obtained was sequenced using 642Un (5′-AAATCAAGAACAAGAAAAAGTGG-3′) and allowed to identify a 1,100-bp sequence. The full 1,576-bp sequence contains a 22-bp 5′ untranslated region and 187 bp of the 3′ untranslated region.

Subsequent mapping was realized in the recombinant inbred line population Térèse × K586 (Laucou et al., 1998) using a cleaved-amplified polymorphic sequence (CAPS) marker. The amplification was realized with primers 198F and 527Dn, and the product was digested using *Sfe*I (Fermentas), cutting the sequence corresponding to the peptidic CTRYAG sequence only in the Torsdag/K586 genotype.

Obtaining the *Psbrc1* Mutant by TILLING Screening

Psbrc1 mutants were identified from an ethyl methanesulfonate population containing 4,800 pea lines using TILLING screening (McCallum et al., 2000). PCR and digestion were performed as described by Dalmais et al. (2008). A 1-kb first amplicon was amplified with primers PsCycN1F (5′-GTCTTGTTCCTGCAGAAGC-3′) and PsCycN1R (5′-GTGCAAGTACATGTTAGAAATGG-3′) at an annealing temperature of 60°C. From this one, a second amplicon of 900 bp was amplified with primers PsCycN2Ftag (5′-ACGACGTTGTAAAACGACCTGCTTCTGGTAAAGGC-3′) and PsCycN2Rtag2 (5′-ATAACAATTTCACACAGGTTTTCCAAGGACTCGTG-3′) at an annealing temperature of 58°C. The gene-specific inner primers carried a universal M13 tail (underlined). To confirm mutations, PCR products were sequenced (GATC Biotech) and sequence analysis was performed (Chromas version 1.4523 software). *PsBRC1* partial genomic sequence and TILLING mutations were integrated in UTILLdb (http://urgv.evry.inra.fr/UTILLdb).

Mutation of the 4654 family was followed using a CAPS marker amplified with primers 4654-8F (5′-GTCTTGTTCCTGCAGAAGCTG-3′) and 4654-317R (5′-CCAAGCTTGAAACTCCTTCAC-3′) and digested with *Tas*I enzyme (Fermentas).

Plant Materials, Growing Conditions, and Phenotype Measurement

Plants used in this study were derived from various cultivars of pea. The *rms1-10* (M3T-884) and *rms4-3* (M3T-946) mutants were obtained in cv Térèse (Rameau et al., 1997). The *rms2-1* allele obtained in Torsdag (Arumingtyas et al., 1992; Beveridge et al., 1997b) was back-crossed in the Térèse background, and BC7 (Térèse × K524) was used in this study. The *Psbrc1* mutant families derived from the TILLING approach were obtained from cv Caméor (Dalmais et al., 2008).

The *Psbrc1* mutant was first back-crossed with its wild-type progenitor Caméor. For the segregation analysis, a BC2-F2 (4654 × Caméor) population was genotyped for the T195I mutation with a CAPS marker (see below) and was phenotyped when plants had 10 leaves expanded. A BC3 mutant line (*Psbrc1*) was used for further study and was named *Psbrc1*^{Cam}. To have a better comparison with the *rms1* mutant used in this study (line M3T-884), the *Psbrc1* mutant was also back-crossed twice in line Térèse (BC2 [Térèse × *Psbrc1*]), and this line was named *Psbrc1*^{Té}. To analyze the phenotype of *rms1 Psbrc1* double mutant plants and compare it with the branching phenotype of single mutants in a comparable genetic background, a cross between M3T-884 (*rms1*) and an

F2 plant (Térèse × *Psbrc1*) that was *Psbrc1* and *afila* (without leaflets, as in Térèse) was done. More than 100 F2 plants were genotyped and phenotyped for *RMS1* and *PsBRC1*, and several F3 families were also analyzed for their branching phenotypes.

For CK quantifications in sap of double mutants, 28 *rms1*, 27 *Psbrc1*, and 40 *rms1 Psbrc1* plants were selected in the F3 generation derived from four F2 (M3T-884 × F2 [Térèse × *Psbrc1*^{Cam}]) plants; these F2 plants were fixed for one mutation and heterozygous for the other one and gave in the F3 generation one-quarter single mutants, one-quarter double mutants, and one-half plants with the same genotype as the parental plant (sap was not collected from the later plants). Approximately 30 wild-type plants from two F2 wild-type plants for both genes were also used as well as the wild-type Térèse, the *rms1* mutant (M3T-884), and the *Psbrc1*^{Te} line.

For genotyping the T195I mutation in *PsBRC1* in the different crosses, a CAPS marker was designed. The amplified PCR fragment using primers 4654-8F (5′-GTCTTGTTCCTGCAGAAGCTG-3′) and 4654-317R (5′-CCAAGCTT-GAAACTCCTTCAC-3′) was digested with *Tas*I enzyme (Fermentas). The CAPS marker for genotyping *RMS1* was based on amplification of the PCR fragment using primers RMS1-118F (5′-TTGGTTGGACTTCACTTTGAGG-3′) and RMS1-984R (5′-CACAACAATCAGCAATGACAGC-3′) and digestion with the *Cfr13*I enzyme (Fermentas).

Plants were grown in pots filled with clay pellets, peat, and soil (1:1:1) supplied regularly with nutrient solution in a heated glasshouse (15°C night and 22°C day) under a 16-h photoperiod (the natural daylength was extended or supplemented during the day when necessary using sodium lamps). For harvesting axillary buds at node 4 or epicotyls, plants were sown individually in 4-dL pots. For longer culture, one or two plants were cultivated per 2-L pot.

Nodes were numbered acropetally from the first scale leaf as node 1. The stage indicated corresponds to the number of nodes with fully expanded leaves.

Hormonal Treatment

The synthetic SL GR24 (kindly provided by F.D. Boyer, Institut de Chimie des Substances Naturelles) was applied on buds as 10 μL of a solution containing 50% ethanol, 1% polyethylene glycol 1450 (Sigma), 0.1% dimethyl sulfoxide (Sigma), and 0.1% acetone containing or not (mock treatment) 500 nM GR24.

The CK BAP (Sigma) was applied to buds as 10 μL of a solution containing 50% ethanol, 1% polyethylene glycol 1450 (Sigma), and 0.5% dimethyl sulfoxide (Sigma) containing or not (mock treatment) 50 μM BAP.

Gene Expression Analysis

RNA Extraction and cDNA Synthesis

Tissue samples were harvested and ground into liquid nitrogen. Total RNA was isolated from 20 to 30 buds or 10 to 15 epicotyls using TRIZOL reagent (Invitrogen) following the manufacturer's protocol. DNase treatment was performed using the Qiagen RNase-Free DNase Set (79254) and the RNeasy Mini Kit (74904) and eluted in 50 μL of RNase-free water. RNA was quantified using NanoDrop 1000 and migrated on gels to check RNA nondegradation. The absence of contamination with genomic DNA was checked using 35 cycles of PCR with *RMS1* primers (see below).

Total cDNA was synthesized from 2 μg of total RNA using 50 units of RevertAid H$^-$ Moloney murine leukemia virus reverse transcriptase (Fermentas) in 30 μL following the manufacturer's instructions with poly(T)$_{18}$ primer. cDNA was diluted 10 times before subsequent analysis.

Real-Time PCR Analysis

Quantitative reverse transcription-PCR analyses were performed using SYBR ROX RealMasterMix (5Prime) with the following specific primers: for *PsBRC1*, *BRC1* forward (5′-AGGCAAGAGAAAGAGCAAGG-3′) and *BRC1* reverse (5′-TTGCATTGCTTTGAGTTTGA-3′ [amplicon of 128 bp]); for *RMS1*, *RMS1* forward (5′-TTGCTCAGGGCTGAACCAAC-3′) and *RMS1* reverse (5′-CACTTCCACACTTGCCACAATC-3′ [amplicon of 113 bp]). Cycling conditions for amplification were 95°C for 10 min, 50 cycles of 95°C for 5 s, 62°C for 5 s, and 72°C for 15 s, followed by 0.1°C s^{-1} ramping up to 95°C for fusion curve characterization. Three biological repeats were analyzed in duplicate. To calculate relative transcript levels, the comparative cycle method based on nonequal efficiencies was used (Pfaffl, 2001). Transcript levels for the different genes were expressed relative to the expression of the *EF1α* gene (Johnson et al., 2006).

CK Quantification

Xylem sap was harvested from roots of 30-d-old plants by applying vacuum to the freshly cut epicotyl with a syringe. Independent pools of 3 mL of sap were used to quantify CKs as described (Morris et al., 2001).

SL Sampling and Analysis

Pea plants were germinated in vermiculite for 6 d and then transferred to aerated hydroponic complete nutrient solution culture, with 12 plants in 6 L of solution in a growth cabinet set at 23°C, 55% relative humidity during the day and 15°C, 65% relative humidity at night, with a 16-h photoperiod and light intensity of 300 μmol m^{-2} s^{-1} provided by cool-white fluorescent lamps supplemented with tungsten lamps. At 19 d after germination, the solution was replaced with water, then 24 h later, batches of 12 plants were transferred to 900 mL of water into which exudate was collected for 24 h. Deuterium-labeled SL internal standards (20 ng each of d_1-orobanchol, d_1-orobanchyl acetate, d_1-epiorobanchyl acetate, d_1-fabacyl acetate, d_6-5-deoxystrigol, and d_6-epi-5-deoxystrigol; all generous gifts of Koichi Yoneyama) were added to each sample. SLs were extracted with 0.6 volume of ethyl acetate, followed by back-extraction with 0.1 M KH_2PO_4. The ethyl acetate fraction was dried with anhydrous $MgSO_4$, filtered, and evaporated to dryness at 35°C. Samples were redissolved in dry acetone, transferred to autosampler vials, redried, dissolved in acetonitrile:water (30:70, v/v), and filtered (0.45 μm) prior to analysis by liquid chromatography-mass spectrometry multiple reaction monitoring (MRM) in positive ion electrospray mode using the Agilent 1100 LC System and an Applied Biosystems Sciex QTrap mass spectrometer. The column was Phenomenex 3 μm C18 Luna 100 × 2 mm, heated to 40°C with a flow rate of 200 μL min^{-1}. The initial mobile phase was 45.5% acetonitrile in 0.1% aqueous formic acid. After 1 min, a linear gradient to 77% acetonitrile over 19 min was applied, then increased to 95% acetonitrile for 3 min. Appropriate MRM transitions were monitored for each labeled standard and corresponding unlabeled SL. For the quantitations reported here, the transitions were mass-to-charge ratio 406 to 232 for d_1-fabacyl acetate and 405 to 231 for fabacyl acetate. Two biological replicates representing pools of 12 plants were analyzed for each genotype. SL content was calculated from MRM peak areas by the stable isotope ratio method.

Statistical Analysis

For the statistical analysis, Student's *t* test and ANOVA were performed using Statgraphics Plus 5.1. Phylogenetic analyses were conducted in MEGA4 (Tamura et al., 2007).

Sequence data from this article can be found in the GenBank/EMBL data libraries under accession number JF274232 for *PsBRC1*.

Supplemental Data

The following materials are available in the online version of this article.

Supplemental Figure S1. Phylogenetic tree of representative TCP proteins.

Supplemental Figure S2. Comparison of branching mutant plant architecture.

Supplemental Figure S3. Grafting experiment.

Supplemental Figure S4. Independent experiments for real-time PCR.

Supplemental Table S1. List of the mutations identified in the *PsBRC1* gene using TILLING.

Supplemental Table S2. Relative expression of *PsBRC1* in different plant organs.

ACKNOWLEDGMENTS

We thank the participants of the ERA-PG COGS project; C. Beveridge, L. Dun, and P. Brewer for helpful discussions; S. Bonhomme, L. Dun, and C.

Beveridge for their comments on the manuscript; and M. Bennett for assistance with the development of SL analysis methods.

Received July 1, 2011; accepted October 28, 2011; published November 1, 2011.

LITERATURE CITED

Aggarwal P, Padmanabhan B, Bhat A, Sarvepalli K, Sadhale PP, Nath U (2011) The TCP4 transcription factor of Arabidopsis blocks cell division in yeast at G1→S transition. Biochem Biophys Res Commun **410:** 276–281

Aguilar-Martínez JA, Poza-Carrión C, Cubas P (2007) *Arabidopsis* BRANCHED1 acts as an integrator of branching signals within axillary buds. Plant Cell **19:** 458–472

Arite T, Iwata H, Ohshima K, Maekawa M, Nakajima M, Kojima M, Sakakibara H, Kyozuka J (2007) DWARF10, an RMS1/MAX4/DAD1 ortholog, controls lateral bud outgrowth in rice. Plant J **51:** 1019–1029

Arumingtyas EL, Floyd RS, Gregory MJ, Murfet IC (1992) Branching in *Pisum*: inheritance and allelism tests with 17 *ramosus* mutants. Pisum Genet **24:** 17–31

Bangerth F (1994) Response of cytokinin concentration in the xylem exudate of bean (Phaseolus vulgaris L.) plants to decapitation and auxin treatment, and relationship to apical dominance. Planta **194:** 439–442

Bennett T, Leyser O (2006) Something on the side: axillary meristems and plant development. Plant Mol Biol **60:** 843–854

Bennett T, Sieberer T, Willett B, Booker J, Luschnig C, Leyser O (2006) The Arabidopsis MAX pathway controls shoot branching by regulating auxin transport. Curr Biol **16:** 553–563

Beveridge C (2000) Long-distance signalling and a mutational analysis of branching in pea. Plant Growth Regul **32:** 193–203

Beveridge CA (2006) Axillary bud outgrowth: sending a message. Curr Opin Plant Biol **9:** 35–40

Beveridge CA, Dun EA, Rameau C (2009) Pea has its tendrils in branching discoveries spanning a century from auxin to strigolactones. Plant Physiol **151:** 985–990

Beveridge CA, Kyozuka J (2010) New genes in the strigolactone-related shoot branching pathway. Curr Opin Plant Biol **13:** 34–39

Beveridge CA, Murfet IC, Kerhoas L, Sotta B, Miginiac E, Rameau C (1997a) The shoot controls zeatin riboside export from pea roots: evidence from the branching mutant *rms4*. Plant J **11:** 339–345

Beveridge CA, Ross JJ, Murfet IC (1996) Branching in pea (action of genes Rms3 and Rms4). Plant Physiol **110:** 859–865

Beveridge CA, Symons GM, Murfet IC, Ross JJ, Rameau C (1997b) The *rms1* mutant of pea has elevated indole-3-acetic acid levels and reduced root-sap zeatin riboside content but increased branching controlled by graft transmissible signal(s). Plant Physiol **115:** 1251–1258

Beveridge CA, Symons GM, Turnbull CG (2000) Auxin inhibition of decapitation-induced branching is dependent on graft-transmissible signals regulated by genes Rms1 and Rms2. Plant Physiol **123:** 689–698

Brewer PB, Dun EA, Ferguson BJ, Rameau C, Beveridge CA (2009) Strigolactone acts downstream of auxin to regulate bud outgrowth in pea and Arabidopsis. Plant Physiol **150:** 482–493

Cline M (1991) Apical dominance. Bot Rev **57:** 318–358

Cline M (1996) Exogenous auxin effects on lateral bud outgrowth in decapitated shoots. Ann Bot (Lond) **78:** 255–266

Crawford BC, Nath U, Carpenter R, Coen ES (2004) CINCINNATA controls both cell differentiation and growth in petal lobes and leaves of Antirrhinum. Plant Physiol **135:** 244–253

Crawford S, Shinohara N, Sieberer T, Williamson L, George G, Hepworth J, Müller D, Domagalska MA, Leyser O (2010) Strigolactones enhance competition between shoot branches by dampening auxin transport. Development **137:** 2905–2913

Dalmais M, Schmidt J, Le Signor C, Moussy F, Burstin J, Savois V, Aubert G, Brunaud V, de Oliveira Y, Guichard C, et al (2008) UTILLdb, a Pisum sativum in silico forward and reverse genetics tool. Genome Biol **9:** R43

Doebley J, Lukens L (1998) Transcriptional regulators and the evolution of plant form. Plant Cell **10:** 1075–1082

Doebley J, Stec A, Hubbard L (1997) The evolution of apical dominance in maize. Nature **386:** 485–488

Domagalska MA, Leyser O (2011) Signal integration in the control of shoot branching. Nat Rev Mol Cell Biol **12:** 211–221

Dun EA, Ferguson BJ, Beveridge CA (2006) Apical dominance and shoot branching: divergent opinions or divergent mechanisms? Plant Physiol **142:** 812–819

Dun EA, Hanan J, Beveridge CA (2009) Computational modeling and molecular physiology experiments reveal new insights into shoot branching in pea. Plant Cell **21:** 3459–3472

Feng X, Zhao Z, Tian Z, Xu S, Luo Y, Cai Z, Wang Y, Yang J, Wang Z, Weng L, et al (2006) Control of petal shape and floral zygomorphy in Lotus japonicus. Proc Natl Acad Sci USA **103:** 4970–4975

Finlayson SA (2007) Arabidopsis Teosinte Branched1-like 1 regulates axillary bud outgrowth and is homologous to monocot Teosinte Branched1. Plant Cell Physiol **48:** 667–677

Foo E, Bullier E, Goussot M, Foucher F, Rameau C, Beveridge CA (2005) The branching gene RAMOSUS1 mediates interactions among two novel signals and auxin in pea. Plant Cell **17:** 464–474

Foo E, Morris SE, Parmenter K, Young N, Wang H, Jones A, Rameau C, Turnbull CG, Beveridge CA (2007) Feedback regulation of xylem cytokinin content is conserved in pea and Arabidopsis. Plant Physiol **143:** 1418–1428

Foo E, Turnbull CG, Beveridge CA (2001) Long-distance signaling and the control of branching in the *rms1* mutant of pea. Plant Physiol **126:** 203–209

Giraud E, Ng S, Carrie C, Duncan O, Low J, Lee CP, Van Aken O, Millar AH, Murcha M, Whelan J (2010) TCP transcription factors link the regulation of genes encoding mitochondrial proteins with the circadian clock in *Arabidopsis thaliana*. Plant Cell **22:** 3921–3934

Gomez-Roldan V, Fermas S, Brewer PB, Puech-Pagès V, Dun EA, Pillot JP, Letisse F, Matusova R, Danoun S, Portais JC, et al (2008) Strigolactone inhibition of shoot branching. Nature **455:** 189–194

Hayward A, Stirnberg P, Beveridge C, Leyser O (2009) Interactions between auxin and strigolactone in shoot branching control. Plant Physiol **151:** 400–412

Hubbard L, McSteen P, Doebley J, Hake S (2002) Expression patterns and mutant phenotype of teosinte branched1 correlate with growth suppression in maize and teosinte. Genetics **162:** 1927–1935

Johnson X, Brcich T, Dun EA, Goussot M, Haurogné K, Beveridge CA, Rameau C (2006) Branching genes are conserved across species: genes controlling a novel signal in pea are coregulated by other long-distance signals. Plant Physiol **142:** 1014–1026

Kapulnik Y, Delaux PM, Resnick N, Mayzlish-Gati E, Wininger S, Bhattacharya C, Séjalon-Delmas N, Combier JP, Bécard G, Belausov E, et al (2011) Strigolactones affect lateral root formation and root-hair elongation in Arabidopsis. Planta **233:** 209–216

Koltai H, Dor E, Hershenhorn J, Joel D, Weininger S, Lekalla S, Shealtiel H, Bhattacharya C, Eliahu E, Resnick N, et al (2009) Strigolactones' effect on root growth and root-hair elongation may be mediated by auxin-efflux carriers. J Plant Growth Regul **29:** 129–136

Kosugi S, Ohashi Y (1997) PCF1 and PCF2 specifically bind to cis elements in the rice proliferating cell nuclear antigen gene. Plant Cell **9:** 1607–1619

Laucou V, Haurogne K, Ellis N, Rameau C (1998) Genetic mapping in pea. 1. RAPD-based genetic linkage map of Pisum sativum. Theor Appl Genet **97:** 905–915

Leyser O (2011) Auxin, self-organisation, and the colonial nature of plants. Curr Biol **21:** R331–R337

Li C, Guevera E, Herrera J, Bangerth F (1995) Effect of apex excision and replacement by 1-naphthylacetic acid on cytokinin concentration and apical dominance in pea plants. Physiol Plant **94:** 465–469

Lin H, Wang R, Qian Q, Yan M, Meng X, Fu Z, Yan C, Jiang B, Su Z, Li J, et al (2009) DWARF27, an iron-containing protein required for the biosynthesis of strigolactones, regulates rice tiller bud outgrowth. Plant Cell **21:** 1512–1525

Liu YG, Whittier RF (1995) Thermal asymmetric interlaced PCR: automatable amplification and sequencing of insert end fragments from P1 and YAC clones for chromosome walking. Genomics **25:** 674–681

Martín-Trillo M, Cubas P (2010) TCP genes: a family snapshot ten years later. Trends Plant Sci **15:** 31–39

Martin-Trillo M, Grandio EG, Serra F, Marcel F, Rodriguez-Buey ML, Schmitz G, Theres K, Bendahmane A, Dopazo H, Cubas P (2011) Role of tomato BRANCHED1-like genes in the control of shoot branching. Plant J **67:** 701–714

McCallum CM, Comai L, Greene EA, Henikoff S (2000) Targeting Induced Local Lesions In Genomes (TILLING) for plant functional genomics. Plant Physiol **123:** 439–442

McSteen P (2009) Hormonal regulation of branching in grasses. Plant Physiol **149:** 46–55

Minakuchi K, Kameoka H, Yasuno N, Umehara M, Luo L, Kobayashi K, Hanada A, Ueno K, Asami T, Yamaguchi S, et al (2010) FINE CULM1 (FC1) works downstream of strigolactones to inhibit the outgrowth of axillary buds in rice. Plant Cell Physiol **51:** 1127–1135

Morris SE, Turnbull CG, Murfet IC, Beveridge CA (2001) Mutational analysis of branching in pea: evidence that Rms1 and Rms5 regulate the same novel signal. Plant Physiol **126:** 1205–1213

Nath U, Crawford BC, Carpenter R, Coen E (2003) Genetic control of surface curvature. Science **299:** 1404–1407

Ongaro V, Leyser O (2008) Hormonal control of shoot branching. J Exp Bot **59:** 67–74

Ori N, Cohen AR, Etzioni A, Brand A, Yanai O, Shleizer S, Menda N, Amsellem Z, Efroni I, Pekker I, et al (2007) Regulation of LANCEOLATE by miR319 is required for compound-leaf development in tomato. Nat Genet **39:** 787–791

Palatnik JF, Allen E, Wu X, Schommer C, Schwab R, Carrington JC, Weigel D (2003) Control of leaf morphogenesis by microRNAs. Nature **425:** 257–263

Pfaffl MW (2001) A new mathematical model for relative quantification in real-time RT-PCR. Nucleic Acids Res **29:** e45

Pruneda-Paz JL, Breton G, Para A, Kay SA (2009) A functional genomics approach reveals CHE as a component of the Arabidopsis circadian clock. Science **323:** 1481–1485

Prusinkiewicz P, Crawford S, Smith RS, Ljung K, Bennett T, Ongaro V, Leyser O (2009) Control of bud activation by an auxin transport switch. Proc Natl Acad Sci USA **106:** 17431–17436

Rameau C, Bodelin C, Cadier D, Grandjean O, Miard F, Murfet IC (1997) New *ramosus* mutants at loci *Rms1, Rms3* and *Rms4* resulting from the mutation breeding program at Versailles. Pisum Genet **29:** 7–12

Rameau C, Dénoue D, Fraval F, Haurogné K, Josserand J, Laucou V, Batge S, Murfet IC (1998) Genetic mapping in pea. 2. Identification of RAPD and SCAR markers linked to genes affecting plant architecture. Theor Appl Genet **97:** 916–928

Rameau C, Murfet IC, Laucou V, Floyd RS, Morris SE, Beveridge CA (2002) Pea rms6 mutants exhibit increased basal branching. Physiol Plant **115:** 458–467

Ramsay L, Comadran J, Druka A, Marshall DF, Thomas WT, Macaulay M, MacKenzie K, Simpson C, Fuller J, Bonar N, et al (2011) INTERMEDIUM-C, a modifier of lateral spikelet fertility in barley, is an ortholog of the maize domestication gene TEOSINTE BRANCHED 1. Nat Genet **43:** 169–172

Ruyter-Spira C, Kohlen W, Charnikhova T, van Zeijl A, van Bezouwen L, de Ruijter N, Cardoso C, Lopez-Raez JA, Matusova R, Bours R, et al (2011) Physiological effects of the synthetic strigolactone analog GR24 on root system architecture in Arabidopsis: another belowground role for strigolactones? Plant Physiol **155:** 721–734

Sachs T, Thimann K (1967) The role of auxins and cytokinins in the release of buds from dominance. Am J Bot **54:** 136–144

Santner A, Estelle M (2009) Recent advances and emerging trends in plant hormone signalling. Nature **459:** 1071–1078

Schommer C, Palatnik JF, Aggarwal P, Chételat A, Cubas P, Farmer EE, Nath U, Weigel D (2008) Control of jasmonate biosynthesis and senescence by miR319 targets. PLoS Biol **6:** e230

Snow R (1937) On the nature of correlative inhibition. New Phytol **36:** 283–300

Sorefan K, Booker J, Haurogné K, Goussot M, Bainbridge K, Foo E, Chatfield S, Ward S, Beveridge C, Rameau C, et al (2003) MAX4 and RMS1 are orthologous dioxygenase-like genes that regulate shoot branching in Arabidopsis and pea. Genes Dev **17:** 1469–1474

Stirnberg P, van De Sande K, Leyser HM (2002) MAX1 and MAX2 control shoot lateral branching in Arabidopsis. Development **129:** 1131–1141

Takeda T, Suwa Y, Suzuki M, Kitano H, Ueguchi-Tanaka M, Ashikari M, Matsuoka M, Ueguchi C (2003) The OsTB1 gene negatively regulates lateral branching in rice. Plant J **33:** 513–520

Tamura K, Dudley J, Nei M, Kumar S (2007) MEGA4: Molecular Evolutionary Genetics Analysis (MEGA) software version 4.0. Mol Biol Evol **24:** 1596–1599

Tanaka M, Takei K, Kojima M, Sakakibara H, Mori H (2006) Auxin controls local cytokinin biosynthesis in the nodal stem in apical dominance. Plant J **45:** 1028–1036

Tatematsu K, Nakabayashi K, Kamiya Y, Nambara E (2008) Transcription factor AtTCP14 regulates embryonic growth potential during seed germination in Arabidopsis thaliana. Plant J **53:** 42–52

Thimann KV, Skoog F (1933) Studies on the growth hormone of plants. III. The inhibitory action of the growth substance on bud development. Proc Natl Acad Sci USA **19:** 714–716

Triques K, Sturbois B, Gallais S, Dalmais M, Chauvin S, Clepet C, Aubourg S, Rameau C, Caboche M, Bendahmane A (2007) Characterization of Arabidopsis thaliana mismatch specific endonucleases: application to mutation discovery by TILLING in pea. Plant J **51:** 1116–1125

Umehara M, Hanada A, Yoshida S, Akiyama K, Arite T, Takeda-Kamiya N, Magome H, Kamiya Y, Shirasu K, Yoneyama K, et al (2008) Inhibition of shoot branching by new terpenoid plant hormones. Nature **455:** 195–200

Wang RL, Stec A, Hey J, Lukens L, Doebley J (1999) The limits of selection during maize domestication. Nature **398:** 236–239

Zentella R, Zhang ZL, Park M, Thomas SG, Endo A, Murase K, Fleet CM, Jikumaru Y, Nambara E, Kamiya Y, et al (2007) Global analysis of della direct targets in early gibberellin signaling in *Arabidopsis*. Plant Cell **19:** 3037–3057

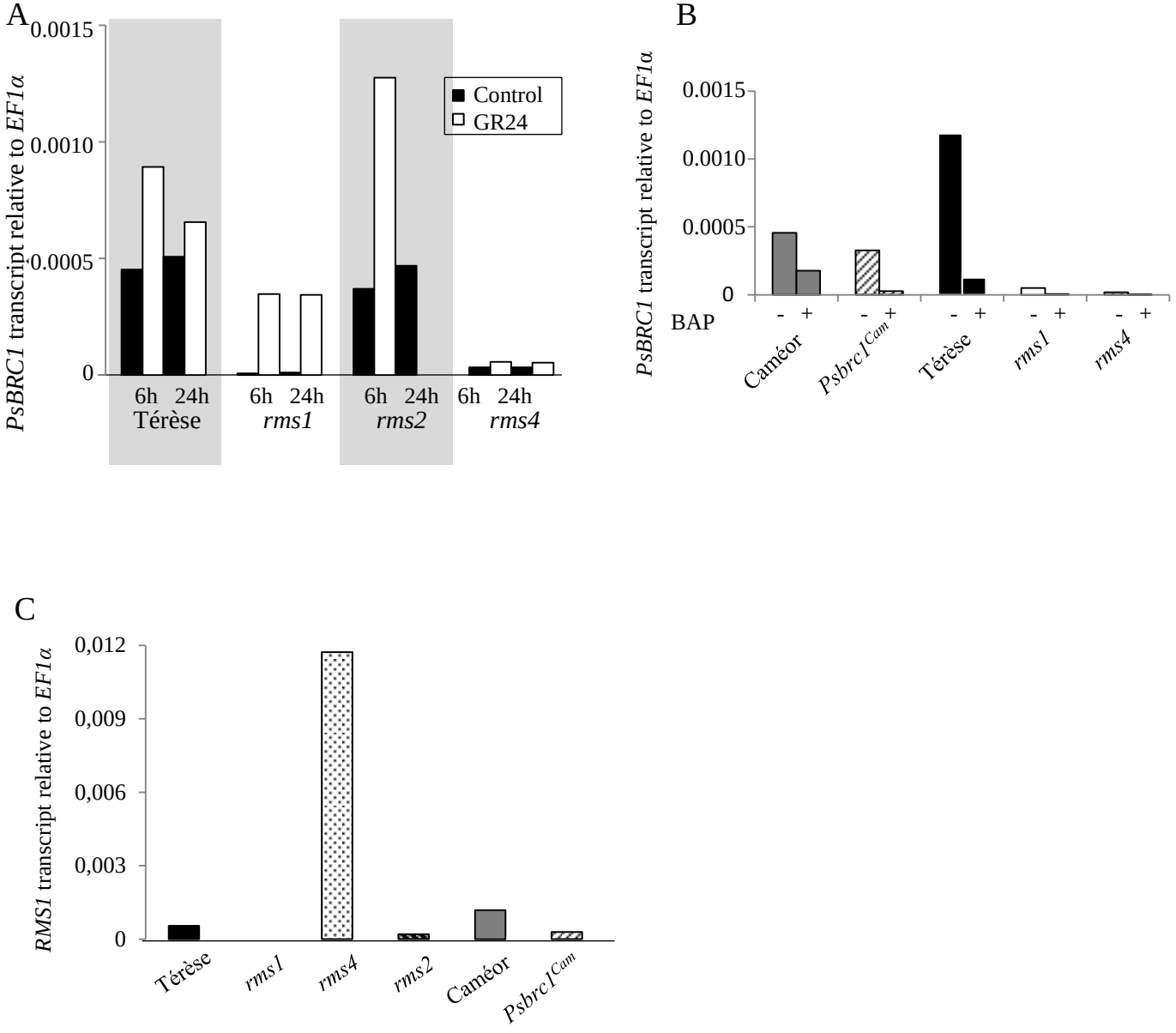

Figure S4. Independent experiments for real-time PCR. A, Effect of GR24 on *PsBRC1* transcript levels. *PsBRC1* transcript levels relative to *EF1α* in axillary bud at node 4 after GR24 applications or mock treated at 6 h and 24 h after treatment of WT Térèse, *rms1*, *rms2* and *rms4* plants. RNA was extracted from dissected buds from pools of 30 plants at the six-node stage and quantified by real-time PCR. B, Effect of BAP on *PsBRC1* transcript levels *PsBRC1* transcript levels relative to *EF1α* in axillary bud at node 4 after BAP (50 µM) applications in WT Caméor, *Psbrc1*^{Cam}, WT Térèse, *rms1* and *rms4*. RNA was extracted from the dissected buds of 30 plants at the six-node stage and quantified by real-time PCR. C, *RMS1* transcript levels in epicotyls of *rms1*, *rms2*, *rms4* and their corresponding WT Térèse and of *Psbrc1*^{Cam} and its corresponding WT Caméor. RNA was extracted from plant at stage 6.

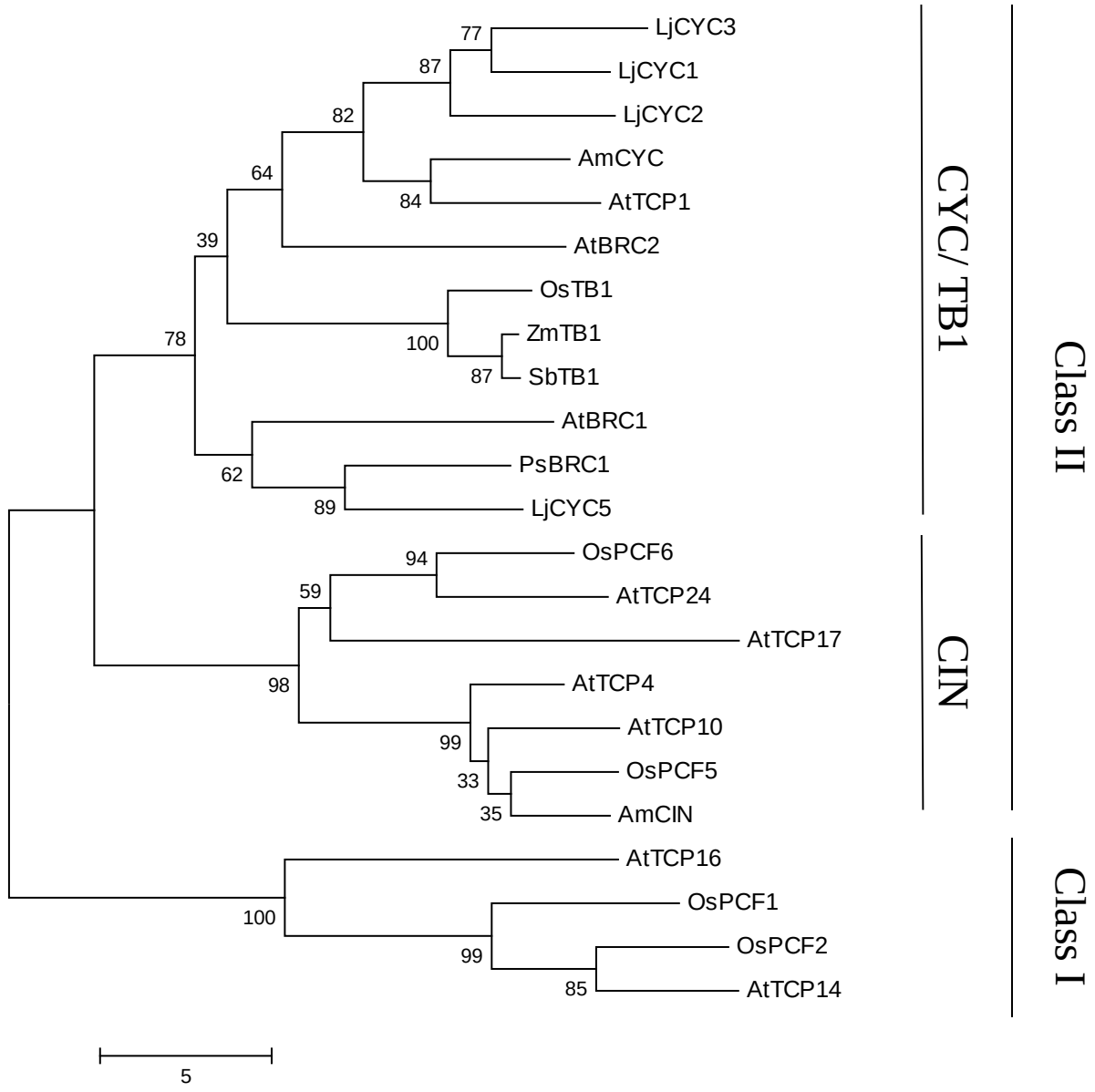

Figure S1. Phylogenetic tree of representative TCP proteins from *Arabidopsis thaliana* (At), PsBRC1 from pea and members of other plant species, *Antirrhinum majus* (Am), *Lotus japonicus* (Lj), rice (Os), maize (Zm), *Sorghum bicolor* (Sb). Evolutionary relationships were analyzed using a selection of predicted amino acid sequences of the TCP domains aligned with the program CLUSTALX (Thompson et al., 1997). The evolutionary history was inferred using the Neighbor-Joining method (Saitou and Nei, 1987) and the optimal tree was generated. Phylogenetic analyses were conducted in MEGA4 (Tamura et al., 2007). Arabidopsis and rice TCP genes named after (Martin-Trillo and Cubas, 2010); LjCYC1, LjCYC2, LjCYC3, and LjCYC5 (GenBank accession nos DQ202475, DQ202476, DQ202477 and DQ202478).

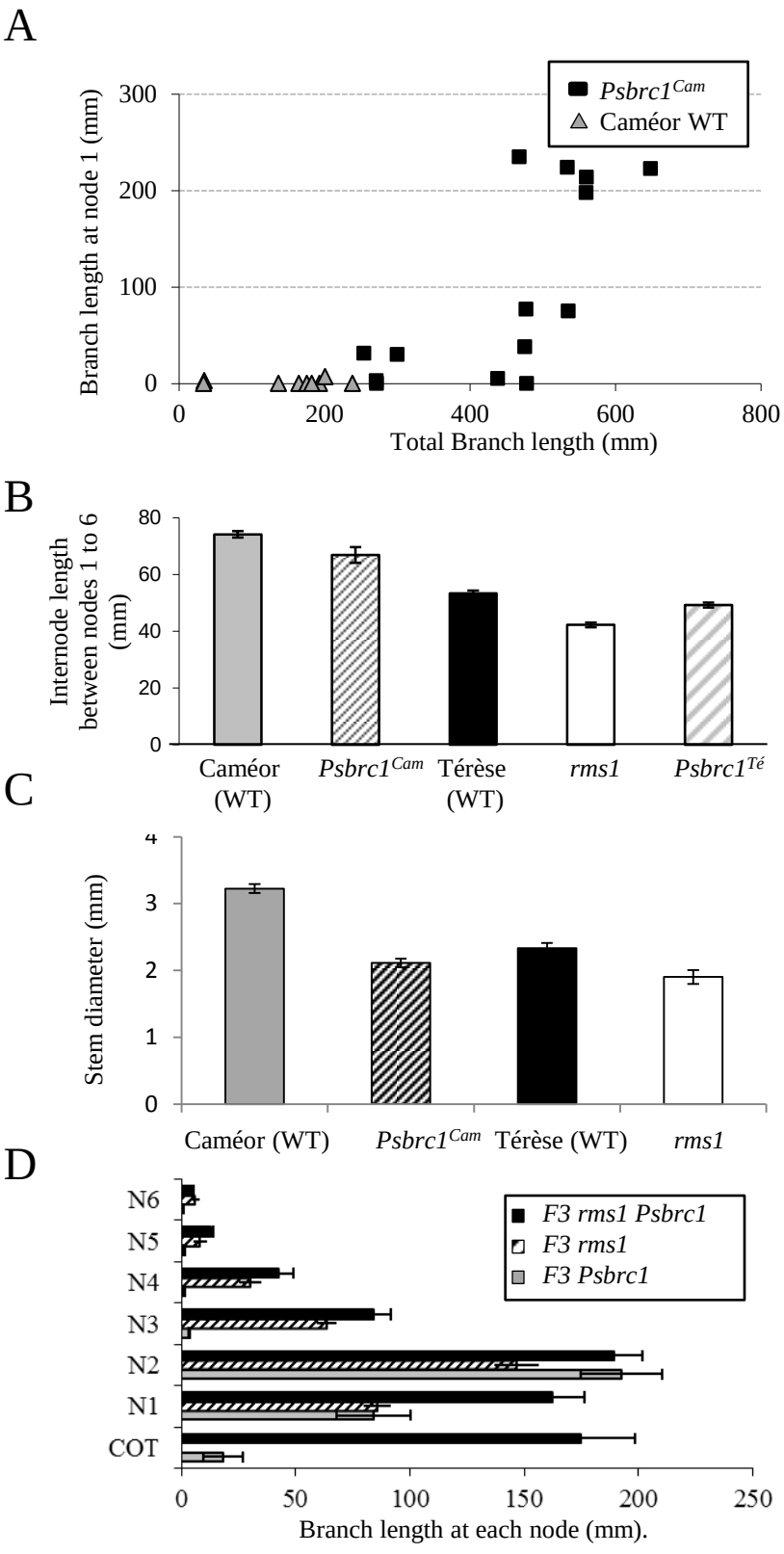

Figure S2. Comparison of branching mutants plant architecture. A, Comparison of branching mutants' plant architecture. A, Branching at node 1 plotted against Total lateral branch length for homozygote *Psbrc1* mutant and WT segregants from a BC2-F2 (4654 x Caméor) population; B, Comparison of internode length between nodes 1 to 6 of WT Caméor, *Psbrc1*^{Cam}, WT Térèse, *rms1* (M3T-884) and *Psbrc1*^{Té}. Data are means +/- SE (n= 12). C, Stem diameter at node 3 of WT Caméor, *Psbrc1*^{Cam}, WT Térèse, *rms1* (M3T-884) plants. Data are means +/- SE (n= 12). D, Branching phenotype of different F3 families from the cross (M3T-884 x (Térèse x *Psbrc1*^{Cam})); 8 individuals per family; means for 6 *Psbrc1* families, 5 *rms1* families and 6 *rms1 Psbrc1* families.

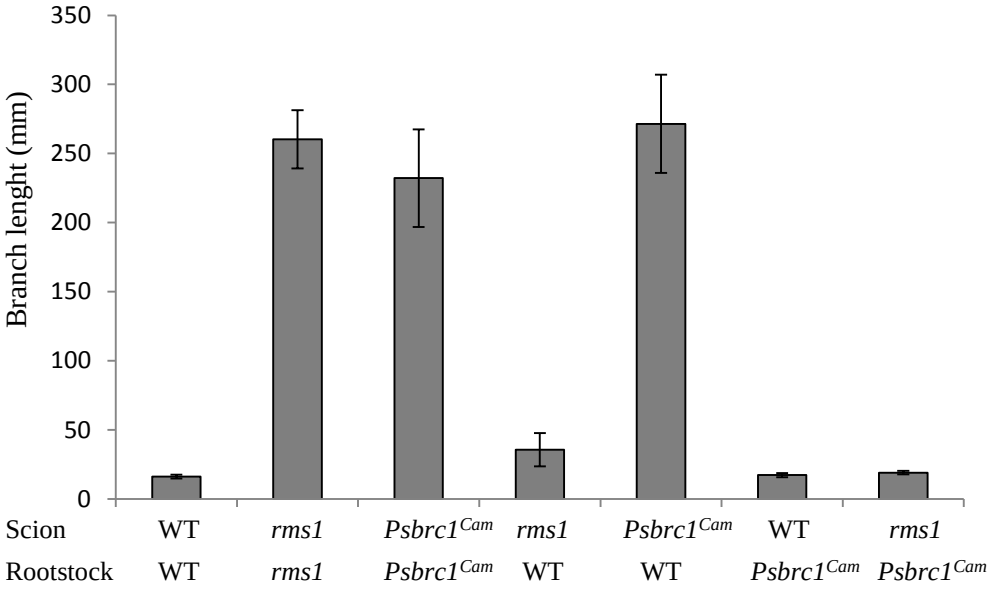

Figure S3. Grafting experiment showing that *PsBRC1* acts in the shoot and that the *Psbrc1*^{Cam} mutant is not strigolactone deficient. Different combinations of grafts between scion and rootstock of 7d-old plants of WT Caméor, *rms1* (M3T-884), and *Psbrc1*^{Cam} as indicated below. Total branch lengths from nodes 1 to 6 were measured 39 days after grafting. Data are means +/- SE (n= 12).